Hyper Spectral Image Denoising: Interscale Orthonormal Wavelet Shrinkage Using Spatial-Spectral Domain

Nitin Bhatia

January, 2010

Hyper Spectral Image Denoising: Interscale Orthonormal Wavelet Shrinkage Using Spatial-Spectral Domain

by

Nitin Bhatia

Thesis submitted to the International Institute for Geo-information Science and Earth Observation in partial fulfilment of the requirements for the degree in Master of Science in *Geoinformatics*.

Degree Assessment Board

Thesis advisor	Dr. Anil Kumar Dr. V.A Tolpekin Dr. A. K Mishra
Thesis examiners	Prof. Dr. V.G. Jetten (Chairman) Dr. Nicholas Hamm (ITC,Member) Prof. Dr. P.K Garg (External Examinar) Sh. P L N Raju (IIRS, Member) Dr. Sameer Saren (IIRS, Member) Dr. Anil Kumar (IIRS, Member) Dr. A.K Mishra (IIRS, Member)

INTERNATIONAL INSTITUTE FOR GEO-INFORMATION SCIENCE AND EARTH OBSERVATION
ENSCHEDE, THE NETHERLANDS
AND
INDIAN INSTITUTE OF REMOTE SENSING
DEHRADUN, INDIA

Disclaimer

Abstract

This research concentrates on developing a noise reduction method using orthonormal wavelet shrinkage to denoise hyperspectral imageries. Hyperspectral imageries, which can be seen as a 3-D array or cube having 2-spatial dimension and one spectral dimension. The spatial and spectral dimensions have different physical property in their respective domains, which is due to the higher degree of regularity in the spatial dimensions than in the spectral dimension. It is therefore important to denoise hyperspectral imageries in both spatial and spectral dimension, separately.

Transformation of image space into mathematical domain provides control on image in terms of operations that can be applied on it. For the purpose of denoising, local approximation is more important than global approximations. The natural tendency of wavelet transform to provide good approximation of local features has proven to be suitable for denoising purpose and hence a choice for this thesis.

In order to speed up the denoising method wavelet subbands are utilized, which reduces the number of spectral curves to be denoised. The reduction in number of curves is achieved by extracting the unique curves and the process is executed in three phases. In the first phase, coefficients representing the image pixels, which belong to the same segment of original image space are recognized and labeled using wavelet subbands. This relationship between pixels and coefficients is obtained by decomposing the subbands LH, HL and HH which is contrary to the custom of decomposing only LL subband. In the second phase, unique spectral curves are produced from the labeled coefficients by projecting the coefficients onto the original image space. Finally, in the third phase the acquired unique spectral curves are denoised using interscale orthornormal wavelet shrinkage.

In order to test the performance of the developed method, HySI (IMS-1) images are used as test images. HySI is a hyperspectral cube with 64 bands & 505m spatial resolution.

To quantify the denoising method performance in terms of Signal To Noise Ratio (SNR) and Mean Square Error (MSE), simulated image is created using spectral libraries. For remote sensing HySI images, because no clean image is available, statistical measures are utilized to test the performance of the denoising method.

The performance of the denoising method is compared with the two state-of-the-art denoising methods, *ProbShrink* approach and *BLS-GSM* approach. The result obtain proves that the developed method performs in the given condition better compared to other denoising methods.

Keywords

Hyperspectral cube, Orthogonal Wavelet Transform, Spatial-Spectral Domain, Segmentation.

Contents

List of Tables

List of Figures

Chapter 1

Introduction

The natural sparse representation, multiresolution analysis, singularity detection capability, dyadic tree interscale relationship etc. has led to the rising popularity of wavelet transform in many signal processing applications [3, 16, 14, 2]. This thesis is about wavelet domain image denoising. The developed method does not postulate any statistical models and estimators to shrink wavelet noisy coefficients. Instead, denoising method parameterized as linear expansion of threshold (LET), which lead to solving linear equations [3].

1.1 Situation and topical outline

"According to C Liu et. al. *Image Noise* is a random variation of brightness information in images produced by the sensor and circuitry of a sensor. Image noise can also originate in the unavoidable shot noise of an ideal photon detector"[1] or from the quantization process while Analog-to-Digital (ADC) conversion [36]. Noise is the most difficult specification of sensor, as it is hard to predict in economically feasible manner.

Noise should not be confused with atmospheric errors. Atmospheric errors are mainly due to the atmospheric constituents (Aerosol, Water Vapors, etc.). On the other hand noise is purely due to the sensor and circuitry involved. These errors will always remain independent of atmospheric constituents [34].

The digital sensors converts the incoming irradiance i.e. the photons coming into the imaging sensor, to analog signal and finally to digital signal. Figure 1 depicts the block diagram of the acquisition process. As observed from the diagram there are mainly five noise components acting on the pipeline namely fixed pattern noise, dark current noise, shot noise, amplifier noise and quantization noise [1].

In remote sensing, during acquisition and transmission of images, external and internal sources often contaminate images with noise, see Figure 1. As mentioned this noise should not be confused with the error induced by the atmospheric constituents such as gases and aerosols, which affect the radiance observed by a sensor and thus, contaminate the observed images [4]. Broadly this affect could also be considered as noise, but more specifically categorized as systematic error.

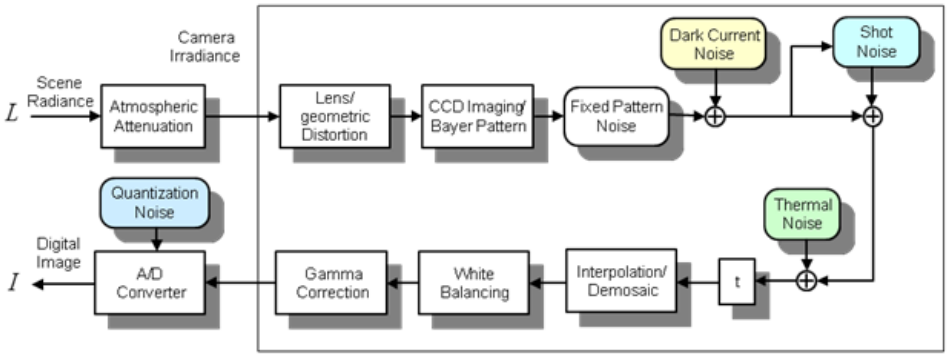

Figure 1.1: Shows the pipeline of image acquisition system.

One way of eliminating noise due to sensors is to design equipments which has minimum noise contribution. But that is another open area of research [1]. In spite of the advances in sensor's design, the acquired data is contaminated with noise which hinders its processing for various applications, videlicet Classification, Segmentation, Compression, Feature Extraction etc.

The denoising method developed in this thesis mainly designed for Gaussian Noise with its standard additive, white, independent model, which is often abbreviated as $AWGN$. $AWGN$ is selected because according to [36, 2] the dominant component in image acquisition system is random noise. The source of random noise is thermal effect of circuit and quantization process [1, 36]. According to center limit theorem, the random noise is Gaussian in nature [36, 35]. The common assumption while selecting the noise model is that the noise variables are independent and have identical distribution (i.i.d).

Due to the fact that noise can not be completely removed from image acquisition system, image denoising methods are employed to suppress the noise up to some level [2]. In general, denoising methods anticipate reducing the noise level or increases the SNR of the observed image, while preserving the image information. In practical scenario, denoising methods impose a compromise between noise reduction and information preservation [2]. Thus, it is not possible to attain zero noise level. Any denoising method can only suppress the noise level to certain extent but cannot completely remove the noise.

One must realize the fact that in image denoising sensor parameters plays important role. The statistics of the noise is not independent from the bands of the image; therefore, assuming some noise model could be approximation only [14, 2]. Ideally, to develop a good denoising method one has to provide the following pre-requisite components to the denoising method:

1. **Noise Level Function (NLF):** Before denoising the image it is important to estimate the noise level, otherwise important image information can be lost [2, 14, 3]. Noise level function does this job by quantifying the noise

level in image. This information is then used by denoising function to denoise the image, so that information is not penalized.

2. **Sensor Parameters**: The sensor parameters help us to generate prior probability for the NLF by simulating the sensor image process [1]. Also, these parameters help us to estimate the missing data, which helps in correctly fitting the NLF curve [1].

Although, using sensor parameters good denoising function can be built, but complexity involved in simulating clean image of the sensor is a *cost ineffective process* [1]. It requires rigorous computation and yet it is impossible to recover the original image [1]. Also, availability of sensor parameters is an issue. Access of sensor parameters is not possible for every user. The reason could be security issues for some satellite or product related policies.

It is therefore very important to explore other methods that can effectively suppress the noise. In this thesis an effort has made to develop denoising method that does not require sensor parameters to denoise the image.

1.2 Image Transformation

There are many domains in which denoising can be done, videlicet image space, feature space or frequency domain. Depending upon the application user can decide which domain is best suited. For example, image space and feature space provide enough information about the image and its characteristics, on the other hand analyzing image in frequency domain enable user to see the different type of frequencies present in the signal [36, 1]. The process is also known as change in basis or image transformation.

The image transformation with basis function gives the characteristics of image or signal in frequency domain, which can not be observed otherwise [18, 36, 14, 2]. Fourier Transform, Wavelets, Ridgelets, etc. are all example of change in basis. Each transformation has its own application and basic characteristic, which should be understood carefully [3, 16, 2]. For example, if the requirement is to analyze the global characteristics of the signal then transformation that uses global functions should be applied, like Fourier transform, which uses sine and cosine functions. On the other hand to locally approximate the signal, Wavelet Transform should be used [36]. Therefore, *It would be wrong to conclude that which transformation is better over other.*

In this thesis wavelet transformation is used to transform the image into wavelet domain. The reason is, wavelet transform based denoising gives good idea about the local features in image, which is important in denoising the image than having global approximations [5]. Also, multiresolution analysis, sparsity or edge detection capability equips the denoising method to handle the noise more effectively in terms of preserving the image information [14, 2, 3]. This only means that wavelet transform can give good approximation of local features, which can be used to remove noise. This motivates us to use wavelet transform to develop denoising method in this thesis. It would be wrong if comparisons of transformation are done without considering the application.

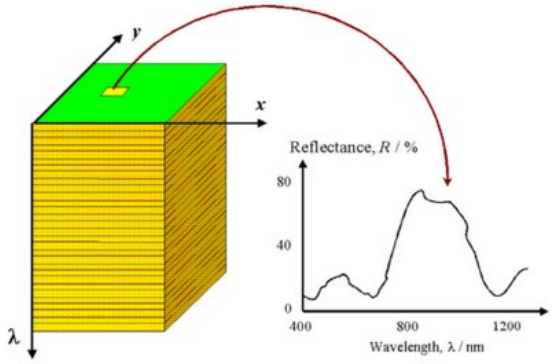

Figure 1.2: Shows the Hyperspectral cube and spectrum.

1.3 Denoising Method

This section gives the sketch for the denoising method. First consideration is which denoising method should be used, then where it should be applied; this specifically refers to spatial-spectral domains and finally how to make this approach computationally efficient. In the following subsections answers to these issues are given.

1.3.1 SURE-LET

Stein Unbiased Risk Estimatation (SURE) can estimate the mean square error without using the clean image [3]. The concept of SURE can be utilized to develop the denoising method. Based on SURE approach many significant researches have been done [7, 3, 16]. To make the SURE function computationaly more efficient, denoising function can be expressed linearly [3]. This linear expression also known as Linear Expansion of Threshold (LET), which can reduce the denoising problem to mere solving the linear equation [3].

1.3.2 Spatial-Spectral Domain

In remote sensing images spatial and spectral domains has significant role, specially when the large number of bands available with narrow bandwidth are available [4]. Spatial domain of the image is the $2-D$ signal and spectral domain is $1-D$ signal. For the image cube they refer to $x,\ y$ and λ directions, see Figure 1.2. It is observed that when both spatial and spectral domains are available, like in the case of hyperspectral cube, both domains should be utilized for denoising purpose [4].

1.3.3 Reduction in number of curves

Using spectral curve to further reduce the noise level improves the results of denoising but at the same time computation time. It is because of large number of spectral curves. The total number of spectral curves to be denoised grows exponentially with increase in size of image [34]. An efficient methodology is

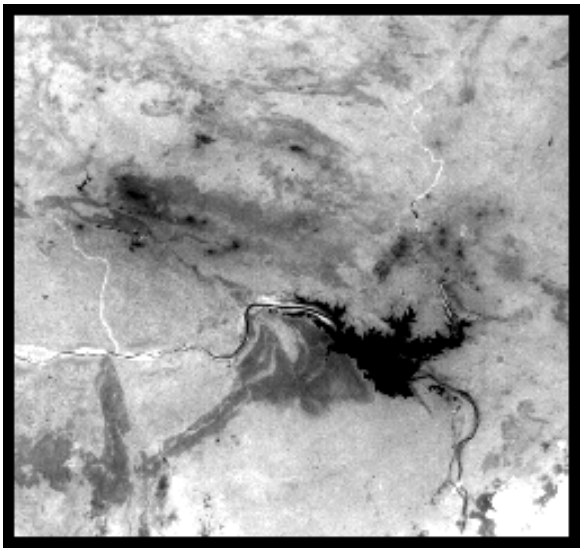

Figure 1.3: Shows the HySi (IMS-1) image (Band-50) of Hirakud Dam Area, Orissa, India.

required that can utilize the spectral domain and at the same time reduce the computation complexity. In this thesis a new segmentation approach is developed that can reduce the number of spectral curves to be denoised. This is achieved by denoising one spectral curve per segment and updating the values of remaining curves with equation.

1.4 Data Set

In this thesis, the developed denoising method is primarily for hyperspectral data. The denoising method is applied to images from Hyperspectral Imager (HySi) that is mounted on Indian Mini Satellite, IMS-1. HySi data has 64 bands ($0.4296\ \mu m$ To $0.956\ \mu m$) with a spectral resolution of better than $15nm$, spatial resolution of $505m$ and radiometric resolution of 12 bit [29].

In order to test the method further for multispectral data the method is applied on OCM sensor mounted on OCEANSAT-1 (IRS P-4) satellite. The sensor has 8 contiguous bands from $0.402\mu M$ to $0.885\mu M$. The radiometric resolution is 12 bit and spatial resolution is $360m$.

In this thesis to check the performance of denoising method simulated image is also used. The simulated image is created using the spectral library available in ENVI 4.4 software. Chapter 3 discusses this point in detail.

1.5 Research Identification

1.5.1 Problem Statement

Hyperspectral remote sensing images are tend to be affected by noise because of narrow bandwidth. Narrow bandwidth reduces the total signal amount that

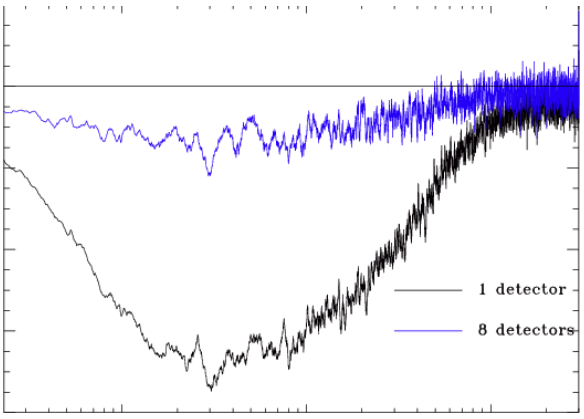

Figure 1.4: Shows the affect of noise on spectral curve.

enters in sensor, thus reducing the signal to noise ratio. Presence of noise in hyperspectral remote sensing images affect the information extraction and scene interpretation [4]. Hyperspectral remote sensing images are mainly used for analysis of surface composition by creating spectral curves [4]. In these spectral curves small trough and crest can change the information about objects, *see Figure 1.4*. Noise affects the hyperspectral images by disturbing the spectral curves and thus the information about objects changes or is lost. In order to make noisy images useful it is important to suppress noise level using denoising methods. Previously attempts were made to develop denoising method for hyperspectral images [4]. But often these methods use sensor parameters to estimate noise level, which may not always available due to various reasons. *Also, computation involved to simulate clean image is cost ineffective, Refer to Section 1 Situation and topical outline, for more detail*. This thesis focuses on the development of denoising method, which do not uses sensor parameters and also suppress noise level effectively.

Processing time of any method is very important component. The aim of this research is not only to develop denoising method which can suppress noise level, but also to increase efficiency in terms of time complexity.

This thesis is set up into two main research objectives and to achieve these objectives, they are divided into research questions. Answer to each research question is a step towards these objectives.

1.5.2 Research Objective

1. To develop a denoising method for hyperspectral data (HySi (IMS-1)) in wavelet domain using SURE-LET method by utilizing spatial and spectral domain with out using sensor parameters.

2. To develop segmentation method that improves the time complexity of the denoising method.

1.5.3 Research Questions

1. What is the suitable wavelet family, support size and vanishing moment for the given wavelet?
2. What is the most suitable decomposition level for the given problem?
3. What is the technical applicability of SURE-LET for hyper-spectral data?
4. What technique should be adopted for reducing the number of spectral curves?
5. How to link the pixels in segments to update their values?
6. Is wavelet family used for denoising and clustering are same?
7. Which validation technique is suitable when no reference image and no sensor parameters are known?
8. How to estimate the noise level when no sensor parameter is available?
9. How to validate the noise level estimator?

1.6 Research Setup

This adopted method is carried out in nine phases: Preprocessing, Transformation into wavelet domain (2-D), Noise estimation, Denoising, Inverse Transform, Segmentation, Transformation into wavelet domain (1-D), Denoising, Inverse Transform.

1.6.1 Phase 1: Preprocessing

In this phase preprocessing of the HySI (IMS-1) cube is done. The output of this phase is the atmospherically corrected image.

1.6.2 Phase 2: Transformation into wavelet domain (2-D)

The atmospherically corrected image is transformed into the wavelet domain using most suitable wavelet family and appropriate vanishing moment.

1.6.3 Phase 3: Noise Estimation

Noise estimation is mainly an estimation of noise level. The estimated noise level is passed to the denoising method, this helps in preserving the image information.

1.6.4 Phase 4: Denoising

In this phase the transformed wavelet coefficients of the noisy image is shrinked using SURE-LET [3] method. This will denoise the image in spatial domain.

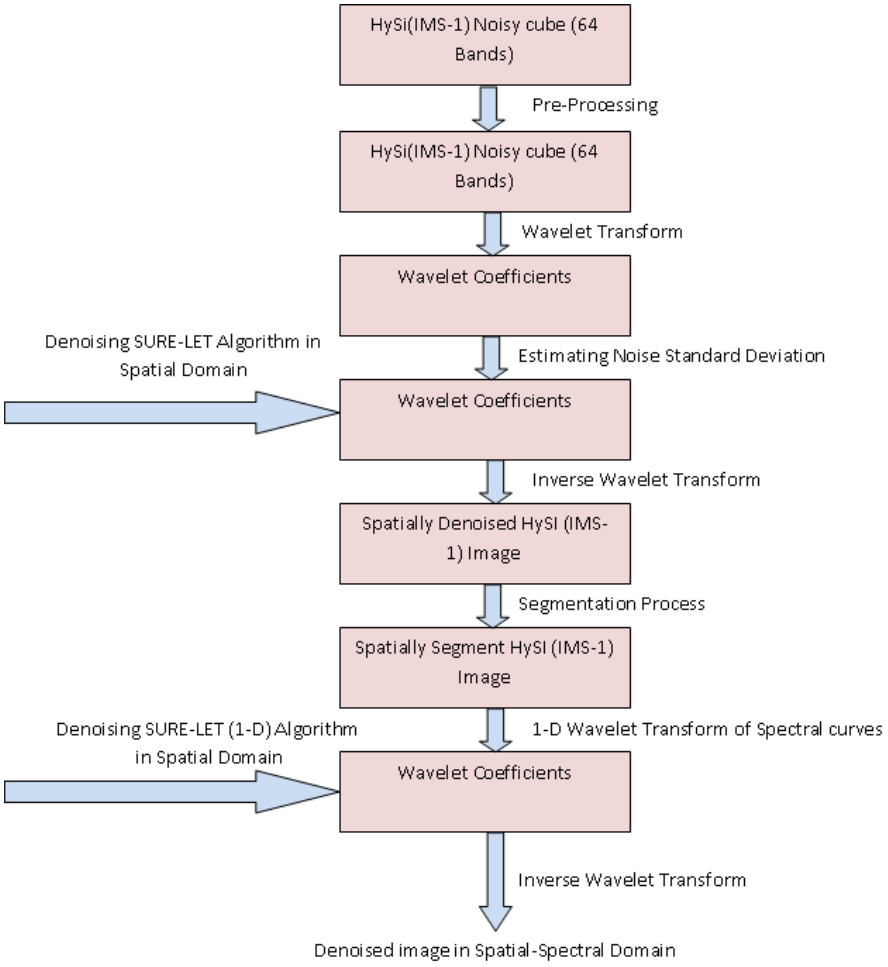

Figure 1.5: Shows the Flow of the research.

1.6.5 Phase 5: Inverse Transform

After denoising the image in spatial domain, the transformed image is set back to original image space. Thanks to the orthogonal property of the wavelet Transform that the same wavelet family with same vanishing moment can be used to take the inverse wavelet transform.

1.6.6 Phase 6: Segmentation

In order to make the denoising method computationally efficient, segmentation of the image is done. This will reduce the total number of spectral curves to be denoised in next phase. It is in this phase, pixels are linked with each other with a mathematical equation.

1.6.7 Phase 7: Transformation into wavelet domain (1-D)

Segmentation process will give us the exact location of the pixel, whose spectrum has to be created, which is representative of the whole segment. After creating its spectrum (1-D signal). This 1-D signal is then transformed into wavelet domain using suitable wavelet family with appropriate vanishing moment.

1.6.8 Phase 8 : Denoising

In this phase the transformed signal is denoised using SURE-LET [3] approach.

1.6.9 Phase 9 : Inverse Transform

After denoising the image in spectral domain the transformed image is set back to the image space using same wavelet family with same vanishing moment that was used to take the wavelet transform (Orthogonal property).

1.6.10 Phase 10: Analysis and Performance measure

In this phase the obtained denoised image is analyzed and its performance is compared with two other state-of-the-art denoising methods.

1.7 Structure of the thesis

The thesis is organized as follows. The thesis contains total nine chapters. In ***chapter one***, Situation and topical outline, the problem statement, the research objectives, the research questions and the approach is described. In ***chapter two***, review of literature on the most relevant aspects for the topic of this thesis is presented. This includes previous works on Wavelet based denoising methods, important developments in wavelet transformation, and previous works on wavelet based segmentation methods. In ***chapter three***, data types and data set used for this thesis and its preprocessing is described. ***chapter four***, is broadly divided into two main parts. In part one brief working of

wavelet based method and noise model is described. In the later part, detailed description of denoising method used for this study is given. ***chaprer five***, is explains the SURE-LET based denoising method. In ***chapter six***, Results of both simulated and remote sensing satellite image is presented. In ***chapter seven***, discussion on the results is given. In ***chapter eight***, conclusion on the results is stated. Finally, in ***chapter nine***, recommendation of this work is given.

Chapter 2

Literature Surveyed

2.1 The Start

"A journey of a thousand miles must begin with a single step." — Lao-Tzu, Tao Te Ching

The history of wavelet theory is very old, but significant work on image processing using wavelets can be witnessed after the classic paper by S.Mallat [5] on the theory of multiresolution signal decomposition by wavelet. According to S.Mallat [5] natural images can be decomposed using low and high pass filters into subbands, which are locally Gaussian and sparse in nature.

Using the same decomposition theory of wavelets another archetypal paper which has quite significant contribution to wavelet based image processing was published by M.Shapiro [6]. According to [6], significant reduction in the image bits can be achieved by zero tree formation of decomposed subband coefficient of an image.

These two papers [5, 6] has mainly revealed the subband relationship and the important statistics of transformed coefficients, which has been used in catering the need of today's image processing challenges.

2.2 The Development

"It is with logic that one proves; it is with intuition that one invents."— Henri Poincar

After the introduction of the above two [5, 6] concepts, significant work in denoising the corrupted images was observed by D.L.Donoho and I.M.Johnstone [7]. Authors' pioneering work to retrieve deteriorated image using wavelet shrinkage has changed the trend of denoising. D.L.Donoho and I.M.Johnstone [7] method, which more commonly known as *soft threshold* aims to minimize the Stein's Unbiased Risk Estimate(SURE) by selecting optimal threshold value, τ_m or universal threshold. This was the improved version of authors' earlier work, *visushrink* , which was based on universal threshold.

SureShrink approach was simple and quite effective. Most importantly it had given new insight to the denoising approach. Since then, many other works has been carried out. The whole work can be seen to develop into two directions.

The first direction focuses on developing the statistics of wavelet coefficients to device statistical models, such as *BayesianShrink* approach which retrieve optimal threshold in Bayesian framework, assuming a generalized Gaussian distribution of transformed coefficients [8].

The second direction work towards on developing the better techniques for wavelet transform, i.e. how efficiently an image can be transformed into wavelet domain. The issues which are most often seen in wavelet transform is shift caused by the filters of DWT. Due to this shift coefficients in parent and child subbands are not aligned to each other in a dyadic tree. In order to align coefficients in dyadic tree shift invariant transform has to be implemented. Work like that done by [9] is an example transforming image into wavelet using shift invariant filters. These authors have shown that transformed coefficients in dyadic tree are aligned to each other if, DWT filters that convolve with the image signal, are invariant to the shift. Other work in this area by [10, 11] better represented the natural images in terms of sparsity of their coefficients.

2.3 The Advances

"All this time, the guard was looking at her, first through a telescope, then through a microscope, and then through an opera glass " — Lewis Carroll, Through the Looking Glass

Based on above two directions, recently, many state-of-the-art techniques emerged. In this section basic idea of these techniques has been explained, also direction on which these techniques emerged has been also covered.

In the year 2002, L.Sendur and I.W.Selesnick [12] presented state-of-the-art work in denoising natural images using wavelets. Their work which is known as *BiShrink* is based on non-Gaussian bivariate distribution of transformed coefficients to model interscale dependencies. The techniques have been developed for both redundant and non-redundant transforms of the natural images.

In the year 2003, a very powerful image restoration technique developed by J.Portilla et. al. [13] emerged. This technique is commonly known as BLS-GSM and developed in both redundant and non-redundant wavelet transform. Their main idea is to provide local statistical description of coefficients in neighborhoods at adjacent position via GSM vector.

In the year 2006, a state-of-the-art technique which devised Laplacian priors for the noise free data emerged. This technique is more commonly known as *ProbShrink* [14] and estimate the probability that a given coefficient has significant information or not [2]. The denoising algorithm is redundant in nature.

Up till now, postulating the statistical models on the transformed coefficients dominated the denoising algorithms[13, 14, 15]. It is in year 2007, a different approach, *new SURE* was proposed. Back in 1995, D.L.Donoho and I.M.Johnstone [7] proposed Stein Unbiased Risk estimate based *SureShrink* approach. Without challenging the original work done by these authors in March 2007 F.Luiser et. al. [3] introduced the powerful approach that directly parameterized the denoising functions as a sum of elementary processes. The method was aimed to reduce the *SURE* risk, which depends upon noisy image alone.

Following the same approach in November 2007 T. Blu and F. Luisier [16] proposed the extension of their original work [3]. In their new method the elementary denoising functions are presented by the linear combinations of these elementary processes. This approach is more generally referred as LET — *Linear Expansion of threshold* . Equipped with SURE principle and LET expansion the powerful algorithm shows better results than many state-of-the-art work [7, 13, 14].

In January 2008, Jose.A et. al [17] introduced the revised method of their earlier work *BLS-GSM* [13]. *BLS-GSM* is one of the powerful methods for image denoising. Its strength lies in its simple and, yet effective local statistics description of oriented pyramid coefficient neighborhoods via GSM vector. But in terms of $L2$ norm its performance is low. To improve their earlier work a coarser adaptation level is introduced, where a neighborhood window size is large in order to estimate the local signal covariance within every subband more effectively.

In May 2008 Buyue Zhang, and Jan P.Allebach [18] proposed the denoising approach also known as ABF. Their method increases the slope of the singularities by transforming the histogram. The ABF method has to optimize the parameters by providing training samples. To provide a training data set input and desired output combinations has to be analyzed, which is not a good approach in case of satellite imageries. In satellite imageries the scene spectral properties induces complexity into the system which can not be easily used for training set. Also, producing training data set required the knowledge of sensor parameters which is not always available. Even after too much of pre-working, the proposed method can not process severely degraded images.

In April 2008, Y. Hel-Or and D. Shaked [19] proposed the denoising method. Although this technique does not require postulating any prior model nor the noise characteristics but it demands the ensemble of example images whose clean and contaminated versions are known as a training set. Working in real time imageries such as satellite imageries, training data set is not always available or not feasible to generate every time.

In this section denoising method and image transformation methods based on wavelets are discussed. With denoising method this thesis also reduces the number of spectral to be denoised and as mentioned in Chapter 1, segmentation approach will be developed. It is therefore essential to learn about developments in image segmentation methods. In the following section work done

on image segmentation is discussed.

2.4 Segmentation

This section briefly introduces the work done in image segmentation in wavelet domain.

In 1979, N.Otsu [20] introduced state-of-the-art segmentation method. Although the method is quite old, but its simplicity, flexibility and power to user does not allow any one to move without acknowledging this work. The method is nonparametric and unsupervised that selects the threshold for image segmentation automatically. According to author, an optimal threshold can be selected by the discriminate criterion, which maximizes the separability of the resultant classes in gray levels.

In 1997, S.G Chang and Martin Vetterli [21] introduced the segmentation method, which uses the characteristic of local Lipschitz regularity. According to their theory, if function f is Lipschitz α at point (x_0, y_0), then its neighborhood point (x, y) can be expressed as:

$$M_s f(x, y) \leq K s^{\alpha} \quad (1) \ [21]$$

In 2001, H.Choi and R.G.Baraniuk [22] introduced the segmentation approach, which is based on multiscale analysis of an image and application of Hidden Markov Models(HMM) on wavelet coefficients to segment the image. Their results were fast as compared to some non-wavelet based algorithms.

In 2003, B.Kim et. al. [23] developed an efficient wavelet based algorithm for image segmentation. Their method utilizes the multi-resolution application of a wavelet transform. According to the author transforming the original feature space into a lower resolution with a wavelet transform provides fast computation of the optimum threshold. Using the multi resolution analysis of the original feature space single or multiple features can be extracted.

In 2004, O.Feron et. al. and H.Snoussi et. al. also used the HMM method to create clusters using wavelet coefficients [24, 25] ,their method uses HMM for the z variable, which extract the different labels to segment the image into different regions.

In 2004, The P.Brault and A.M Djafari extended the approach of [24, 25] by introducing PMRF modelling in spatial domain. This method incorporated the spatial context of pixels and its neighbors to improve the results.

In 2005, M.Figueiredo [26] introduced segmentation method, which allows using wavelet-based priors for image segmentation. Their method can be used in supervised, unsupervised, or semisupervised modes. The method exploits the ability of wavelet-based priors to model piece-wise smoothness and the computation efficiency of fast algorithms for wavelet-based processing.

In 2006, A.Ertrk et. al. [27] developed method for hyperspectral image segmentation. Their approach is focuses on the phase-correlation measure of subsampled hyperspectral data. According to the author sub sampling of hyperspectral data spectrum can provide robustness against noise and spatial variability. On the subsampled data set applying phase correlation can determine spectral similarity. Segments are generated by extracting the similar and dissimilar pixels, which are decided according to the peak value of the phase correlation.

In 2008, D.Benot et. al. [28] developed a method to extract the real-time description, position and size, of liver vessels from 2D ultrasound images. The method is implemented in two $phases$. In $phase1$ seeds points are defined by using scale-space theory of rough localization of the vessels. In the second $phase$, analysis of 1D wavelet transform is done for detecting the vessel contours. According to the author, the size of the vessel can then be computed by fitting ellipses on the edge points.

In this section we have seen the developments in segmentation method. It is observed that natural tendency of wavelet transform can be used to develop a good segmentation method.

Chapter 3

Data Set and Pre-Processing

This chapter discusses about the data sets used in this thesis and the pre-processing these data sets. Also, brief reviews of the possible reasons of the presence of noise in these data sets have been presented. In this research work following three types of data sets is used:

1. **HySi (IMS-1)**
2. **Simulated Image**
3. **OCM (OCEANSAT-1)**

The preceding sections discusses about the above mentioned data sets. Section 3.1 discusses about HySi (IMS-1) sensor, information about the scene, pre-processing steps and the possible reasons of noise, section 3.2 discusses about the generation of simulated image and how and why noise is added in it, section 3.3 discusses about the OCM sensor and the type of noise present in it.

3.1 Hyperspectral Remote Sensing Data

As mentioned in the chapters 1 the denoising method developed in this thesis is primary for hyperspectral data set. In the following sub-section, detailed review about the hyperspectral data set used is present.

3.1.1 About Hyperspectral Imager, HySi (IMS-1)

On April 24, 2008 India launched Indian Mini Satellite, with two payloads: Multispectral Camera (Mx) and Hyperspectral Imager (HySI). In Table 1, the orbital specification of the satellite is given.

Hyperspectral imager (HySI) is a hyperspectral sensor from visible to near infrared in 64 contiguous spectral bands. The capability of the sensor to resolve the spectral region, from 0.4 to 0.92μ m, is 15 nm. The sensor is a coarse imaging instrument with spatial resolution $505m$. The radiometric resolution of the sensor is 12-bit, which when quantized; generate the 64-band data with 12-bit levels (quantization).

Table 3.1: Shows the orbital specification of IMS-1 satellite (Source: http://www.nrsc.gov.in/ims-1.html

Orbit	Polar sun-synchronous
Orbital Altitude	626 km
Semi major Axis	7004.281 km
Eccentricity	0.001 degrees
Inclination	97.999 degrees
Local time	9.30 AM (descending node)
Orbits/day	14.79
Local time	9.30 AM (descending node)
Repetivity	355 orbits in 24 days
Period	97.36 minuites

3.1.2 Scene Information

In this thesis, scene of the HySI image of the Hirakud Dam Project has bee used. This dam is built across river Mahanadi at about 15 Kms, upstream of Sambalpur town in State of Orissa, India (Lat = 23.93N, Lon = 84.20 E). Figure 3.1 shows, the 256×256 pixels image of the HySI, at $0.8399\mu m$ wavelength or 50th band.

In the Figure 3.1, the water body observed is the largest dam of India, Hirakud Dam. This area plays a very significant role in validation of denoising method. With 505 m spatial resolution and considering the depth of the dam, in later chapters, the standard deviation of this area is used to measure the improvements in the SNR of the image. This measure is a strong validation criterion used in this research, explained later in the chapter.

3.1.3 Presence of noise

The HySI images are highly contaminated with noise. Although the affect of noise can be seen on all the bands, but in first fifteen bands, from 0.4296 to $0.539\mu m$, the noise level is very high such that hardly any object is visible. In other words, there is hardly any information present. Table 3.3 shows, the presence of noise in different wavelengths of the HySI. From the visual analysis

Table 3.2: Shows the specification of HySI sensor (IMS-1) (Source: http://www.nrsc.gov.in/ims-1.html

Parameter	**Value**
Swath (km)	130
Spatial resolution (m)	505.6
Spectral range (microns)	$0.4 - 0.95$
Quantization (bits)	12
Data rate (Mbps)	4.0
Repetivity (days)	24 days

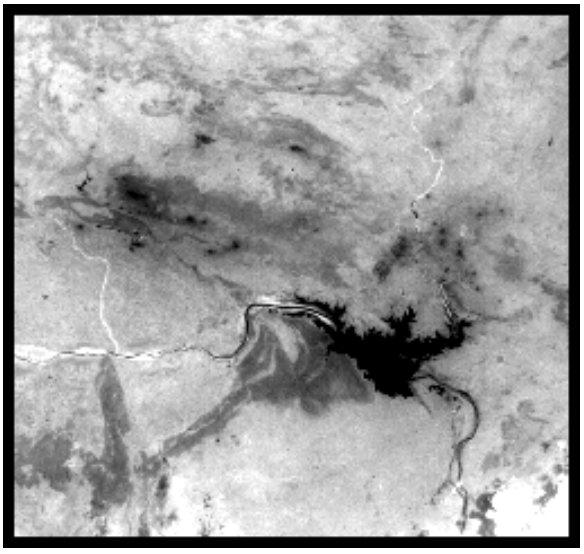

Figure 3.1: Shows the HySI image of the Hirakud Dam Project built across river Mahanadi at about 15 Kms, upstream of Sambalpur town in State of Orissa, India (Lat = 23.93N, Lon = 84.20 E).

it can be concluded that the noise is *more dominating in intial wavelengths (* 0.4296 *to* $0.539\mu m$*) and at the end, near* $0.9312\mu m$*wavelengths*, *see Band 1,8,12 and 64 in Table 3.3*. The in between spectral bands are comparatively less contaminated with noise, *see Band 35,45 and 50 in Table 3.3*.

There are mainly two types of noise affecting the HySI images, which are as follows:

1. **Low Saturation Radiation :** The affect of this noise can be seen in initial wavelengths (0.4296 to $0.539\mu m$), *see Band 1,8,12 in Table 3.3*. From these images it can be observed that the SNR content is very low, which means the signal content reaching the sensor was very small.

2. **Sensor Noise**

   (a) **Low Bandwidth :** In hyperspectral data the bandwidth of the spectral bands are very narrow. With the contiguous spectra of hyperspectral cube the 1-D spectrum for a particular class can be plotted. This spectrum according to spectrography theory has unique characteristics for different features [4]. These characteristics curves can extract different features, which is not possible for the multispectral imageries. But this comes at the cost of problem of low SNR, specifically in some wavelengths. The narrow bandwidth does not allow entering more signals to the sensor.

   (b) **Sensor circuitry :** As mentioned in section 1 of Chapter 1 that many types of noise affect the images during the acquisition process, *see Figure 1.1*

3.2 Simulated Data Set

This section discusses about the need to generate simulated image, how it is generated, and addition of noise in it.

3.2.1 The Need

The very challenge of the denoising methods is the measurement of accuracy or performance of the method developed. The most accurate measures and usually used measures to check the accuracy of any method is mean square error (MSE) and signal to noise ratio (SNR) or peak signal to noise ratio (PSNR) [2, 18].

The MSE of a method is a way to measure the difference between an estimated / calculated and the original value of the image. In other words, "MSE is an estimation of a risk, corresponding to the expected value[3]". MSE measures the average of the square of the "error." [16]. Following is the equation to calculate the MSE of any method:

$$MSE(\theta^{\epsilon}) = E[(\theta^{\epsilon} - \theta)^2] \tag{3.1}$$

$Where,\ \theta^{\epsilon}\ is\ an\ estimated\ value\ of\ \theta\ E[]\ is\ the\ estimation.$

Looking carefully at Equation (3.1) it is observed that in order to calculate the MSE, access to θ, i.e. to original image is required. In case of denoising, the original image is referred to as clean image or image without any noise or with true brightness value. In case of remote sensing satellite image acquisition system access to clean image is not possible. Even with the help of sensor parameters only simulated true image can be generated, which again has some error in it [1].

Another measure to check the performance of denoising method is PSNR, which measures the peak or maximum power of a signal and the power of noise. PSNR can be expressed with the following expression:

$$PSNR = 20 \cdot log_{10}\left[\frac{MAX_i}{MSE(\theta^{\epsilon})}\right] \tag{3.2}$$

Equation 3.2 demonstrates the requirement of MSE to calculate PSNR and ultimately the requirement of clean image. Thus, without having the clean image MSE or PSNR can not be computed.

To tackle with the above problem following two solutions are presented:

Simulated image with other sensor's data can be generated. If there exist data set, which has spectral bands at all wavelengths that noisy data set has, then this data set can generate simulated image from its corresponding wavelengths.

To accurately produce the simulated image from other data set require answering following challenges:

1. **Scene :** The scene of the two data set should match, then only the sub set of bands can be taken.

2. **Time :** Significant amount of shift in spectral values can be observed with change in time, which is commonly referred to as temporal changes. The two data sets are therefore required to be taken at same time/period of the year.

3. **Altitude and spatial resolution :** There should not be much difference in the altitude and spatial resolution of the two data sets.

Though not impossible, but to meet all the above conditions is a daunting task. The scene and temporal requirement can be easily matched but the altitude and spatial resolution for the same or higher spectral resolution is little difficult. This is because usually, satellite agencies launch new satellite with some modifications in it.

3.2.2 How to produce simulated image

In this research work, to meet the challenges mentioned in last sub-section, theory of remote sensing is used. *" An apple will be an apple will be an apple!! "*, the spectral value of the pure classes does not change (much) with the change in the sensor [34]. For example, the spectral value of deep water body will have little change with change in sensor, assuming the data set is atmospherically corrected.

Note: This theory is valid only when dealing with multispectral-multispectral data set or hyperspectral-hyperspectral(with not much difference in band numbers) data sets, but not for multispectral-hyperspectral data sets. The spectral values of an object can not be compared in multispectral data set and hyperspectral data set. " Compare apple with an apple!!"

With this idea, the simulated image is created by following two steps:

1. **Extract pure Classes :** In this step, the pure classes from the images are extracted. Expert users can extract these classes by visual interpretation. Usually, water, forest, dry river bed or settlements are easy targets.

2. **Spectral library signatures :** Once the pure classes present in the scene are identified, the corresponding class spectra and its spectral values can be picked from the spectral library. These values can then directly be used as pixel values for all the corresponding bands or wavelengths.

In this research work, following the above two steps simulated image is created such that there exist four classes in each band. These classes are as follows:

1. Agriculture

2. Forest

3. Water

4. Fallow Land

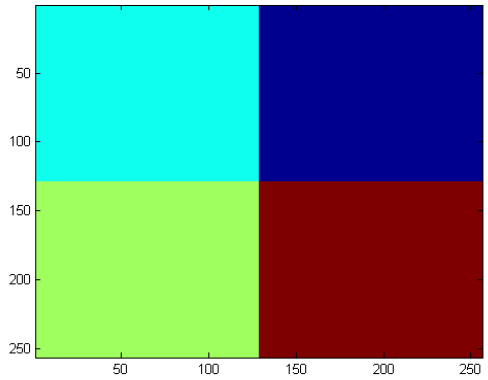

Figure 3.2: Shows the simulated image with four classes.

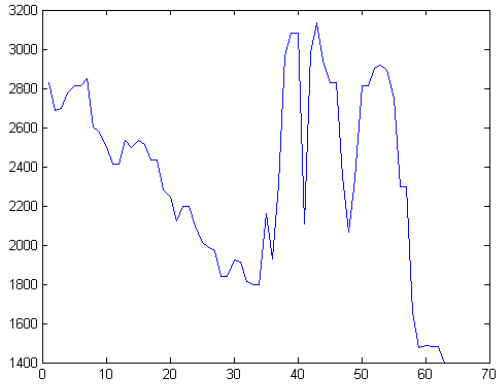

Figure 3.3: Shows the spectral plot for agriculture class.

Note: In this thesis, ENVI 4.4 spectral library is used. Figure 3.2, 3.3 and 3.4, shows the simulated image and the spectral plots of the Forest and Agriculture class

3.2.3 Adding Noise to the simulated image

In order to check the performance of denoising method the noise of known decibel levels (db) have been added. This will provide two data sets, noisy and clean. The denoising method is then applied to the noisy data set and its performance is measured using clean, noisy and denoised versions.

To add the known noise in the simulated data, set following equation is used:

$$Xnoisy = SynImage(:,:) + randn(256, 256) * NoiseStd \tag{3.3}$$

$Where,\ Xnoisy\ is\ noisy\ data\ set, SynImage\ is\ smulated\ image\ ,$

$randn(256, 256)\ is\ MATLAB\ function\ to\ generate\ random\ values\ of size\ 256\times 256\ and$

$NoiseStd\ is\ the\ standard\ deviation\ of\ noise.$

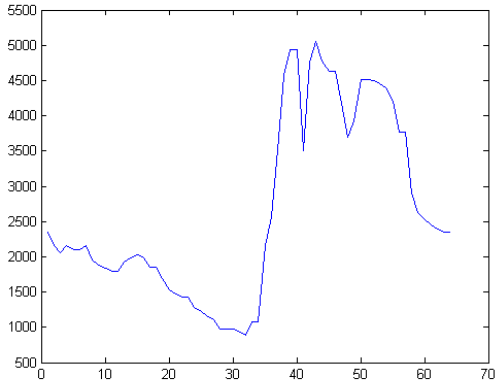

Figure 3.4: Shows the spectral plot for forest class.

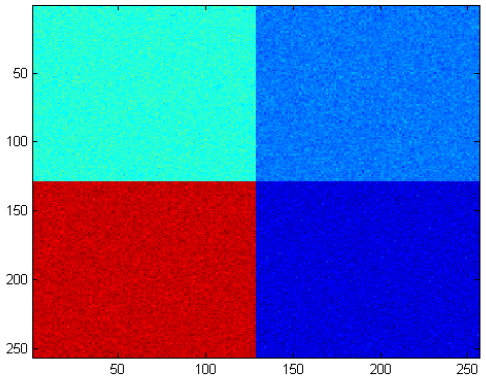

Figure 3.5: Shows the noisy simulated image after adding noise of 60 Std to the clean simulated image.

Figure 3.5 and 3.6 shows the noisy simulated image and noisy spectral plot of the agriculture class.

Table 3.3: Shows HySI Band 1, 8, 12, 25, 50, 64

Band Number	Image	Band Number	Image
Band 1	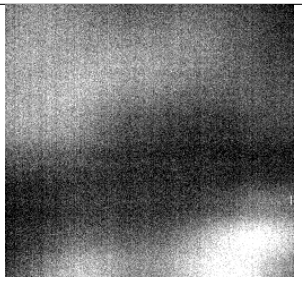	Band 8	
Band 12		Band 25	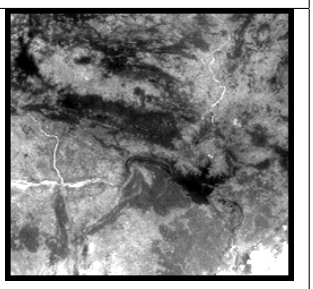
Band 35	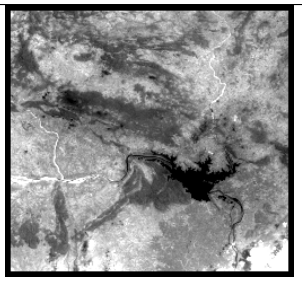	Band 45	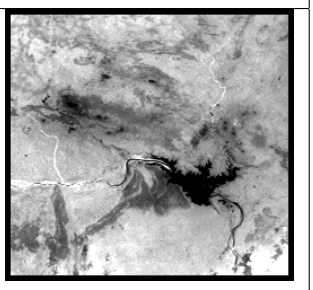
Band 50	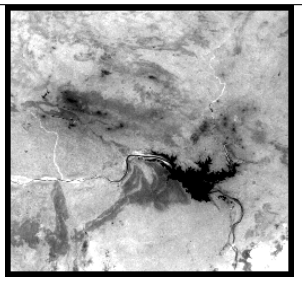	Band 64	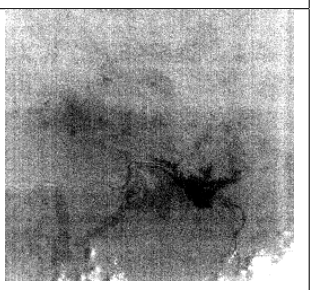

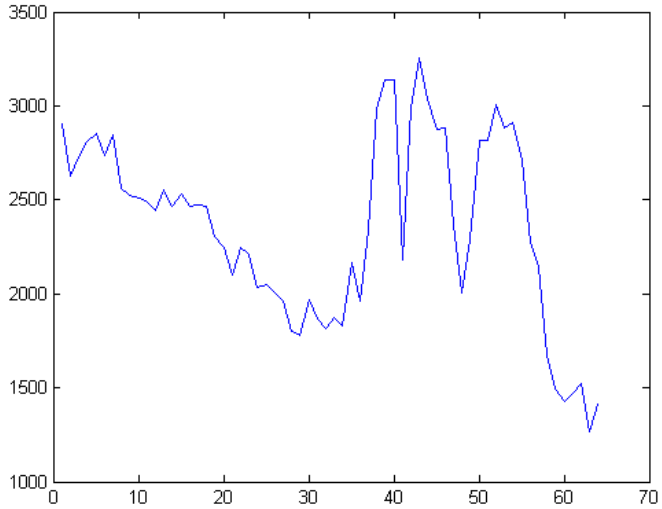

Figure 3.6: Shows the noisy spectral plot of agriculture class.

3.3 Pre-Processing

The image acquisition system of satellite remote sensing has large interference due to atmospheric particles through absorption and scattering of the radiation from the earth surface [4]. Before applying the denoising method to the noisy data it is essential to remove these atmospheric effects [4]. Applying denoising without removing the effect of the atmosphere can not give good results, because the denoising method will try to remove the effect of atmosphere considering it as a random noise. Although, there is no harm for denoising method to do so, but the problem is there is no one solution to atmospheric error. As said before, atmospheric effect is due to the atmospheric particles, which has different composition and density in different regions and in different period of the year. It is because of this reason different atmospheric correction models are developed, which consider these variability [4].

After correcting the data set for atmospheric corrections, only sensor noise remains and thus, simplifies the task of denoising by restricting it to deal with only sensor based noise. In practical scenario, assuming that atmospheric correction will completely remove the atmospheric effect is wrong!! Models used to correct this effect are an assumption. In order to completely remove the atmospheric effect of all the parameters, such as aerosol concentration, water vapor concentration; time of flight etc. should be very precisely known. What best can be done is to have a close approximation of the environment in which image is taken. Due to this uncertainty 20% to 30% atmospheric noise does not wipe out from the corrected data set.

In this thesis, **ENVI 4.4 FLAASH** software is used to correct the **HySI data set**. Input to the package is a radiance image and setting of parameters. Some of these parameters are:

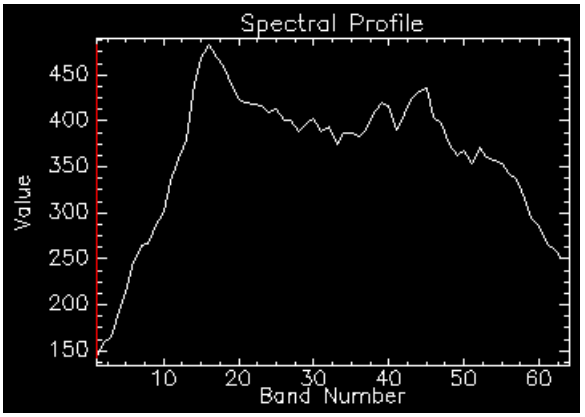

Figure 3.7: Shows the z-profile without correcting the atmospheric effect.

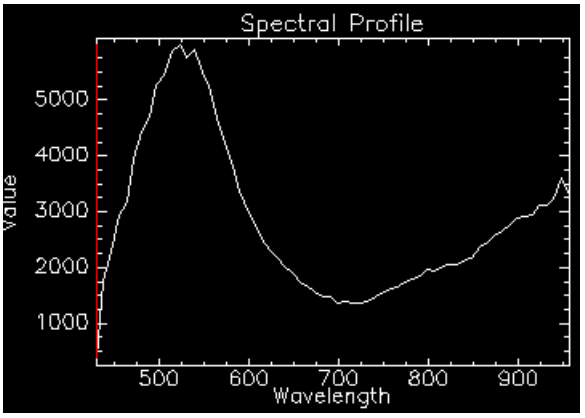

Figure 3.8: Shows the z-profile after correcting the atmospheric effect.

1. Scene Lat Lon.
2. Altitude of sensor.
3. Number of bands.
4. Aerosol, Water Models.
5. Correction model.

In Figure 3.6, 3.7 the improvement in data set can be viewed. The atmospheric correction becomes more important when dealing with hyperspectral data. In hyperspectral data spectral profile of the features are mainly used to discriminate between two features. Sometimes this difference is very small. Due to atmospheric effect the small crest or trough are shadowed or not visible under the high energy received from atmosphere [4].

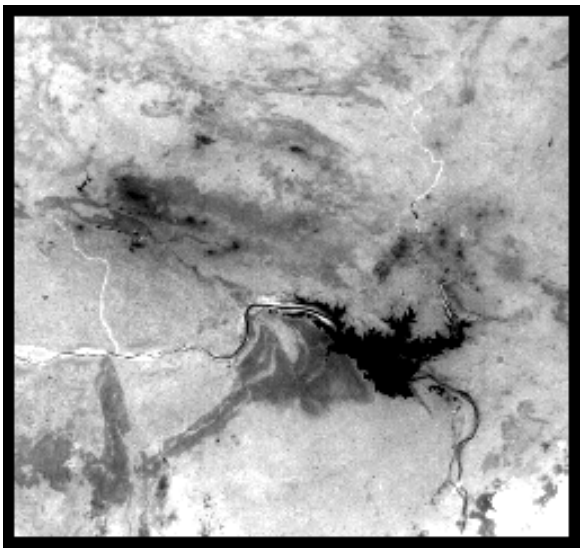

Figure 3.9: Shows the HySI Band 50 image after correcting the atmospheric effect.

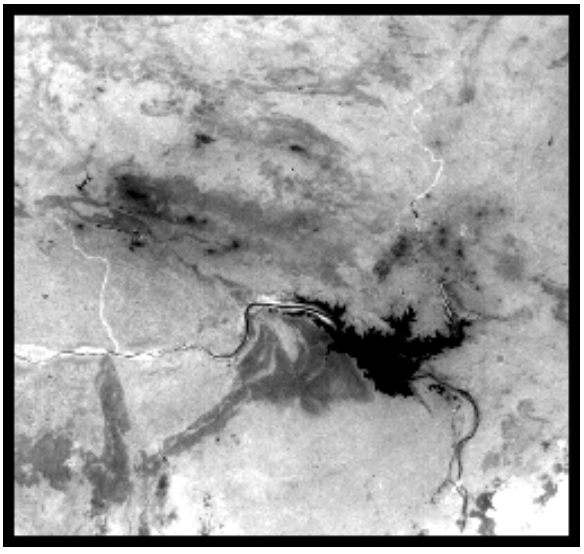

Figure 3.10: Shows the HySI Band 50 image with out correcting the atmospheric effect.

3.4 Multispectral Data set: OCM

In order to test the performance of the denoising method on multispectral data set, Ocean Color Monitor (OCM) sensor's data is used. OCM sensor is mounted on OCEANSAT-1 (IRS P4). OCM sensor is designed to serve the applications in the area of oceanography [29]. OCM sensor operates in the visible and near infrared (NIR) in eight bands. Following is the band information of the OCM sensor:

1. **Band 1:** Band 1 is at the wavelength $0.402\mu m$.
2. **Band 2:** Band 2 is at the wavelength $0.433\mu m$.
3. **Band 3:** Band 3 is at the wavelength $0.480\mu m$.
4. **Band 4:** Band 4 is at the wavelength $0.500\mu m$.
5. **Band 5:** Band 5 is at the wavelength $0.545\mu m$.
6. **Band 6:** Band 6 is at the wavelength $0.660\mu m$.
7. **Band 7:** Band 7 is at the wavelength $0.745\mu m$.
8. **Band 8:** Band 8 is at the wavelength $0.845\mu m$.

The sensor was successfully launched on 26th, May 1999, to provide monitoring of the ocean surface at 720 km altitude with $360m$ of spatial resolution. The sensor is designed so as to give the high radiometric performance of 12 bit.

In this thesis, scene of the OCM image of the Goa located on the west coast of India (Lat = 15 25' N, Lon = 73 43' E) is used. Figure 3.11 shows, the 256×256 pixels image of the OCM, at $0.845\mu m$ wavelength or 8th band, of the mentioned scene.

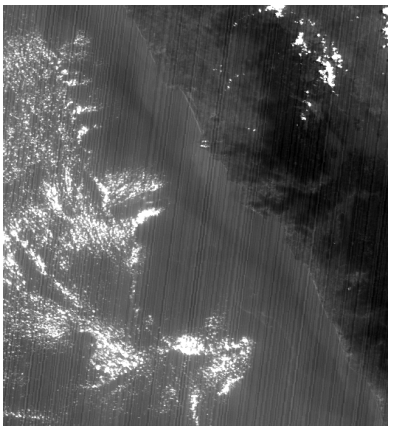

Figure 3.11: Shows the OCM image of the Goa located on the west coast of India (Lat = 15 25′ N, Lon = 73 43′ E).

Chapter 4

Factors influencing the development of denoising method

In this chapter, factors which have a significant impact on developing the denoising method is discussed. The subsequent sections discuss 'the general steps for any denoising methods', 'need to change of basis', 'the gains using wavelet', 'comparison with other transformation technique' and in last section 'noise model' is reviewed.

4.1 General steps for any denoising method

Broadly denoising methods can be designed into three main steps:

1. **Identify domain**, This step suggests the domain, where denoising method can be applied. This can be image space or frequency domain.
2. **Design denoising algorithm**, Based on the domain on which denoising method is to be applied and the type of noise it tackles, denoising method is designed. When dealing with remote sensing images with multiple bands, spatial-spectral information can also be used.
3. **Estimate noise level**. The main input to any denoising method is the estimation of noise level present in images. This estimation is the crux of any denoising method and should be properly designed. Especially, for remote sensing images, where image information and noise, changes with wavelength.

4.2 Importance of change in basis for denoising

4.2.1 What is change in basis?

Chapter 1, section 1.2 discusses about the change of basis, which is also popularly known as transformation image space into frequency domain. In this

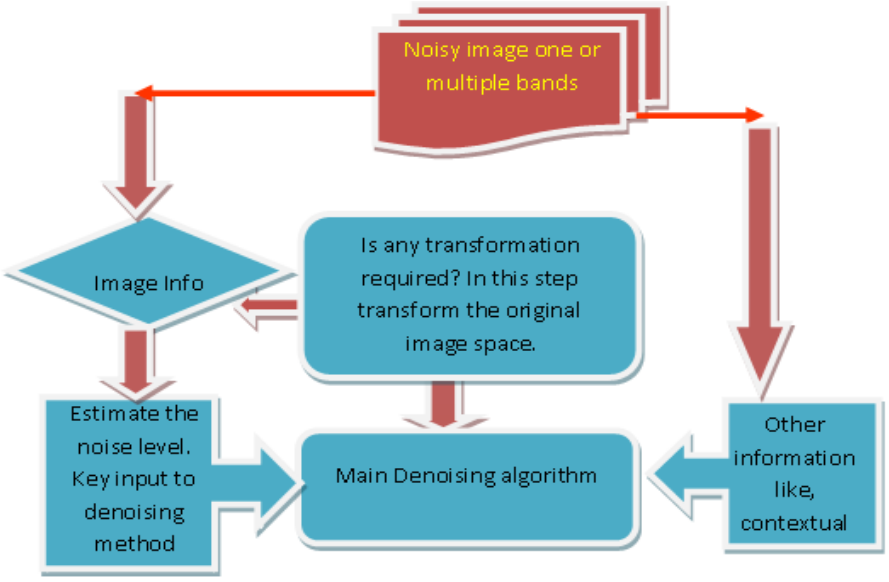

Figure 4.1: Shows the general block diagram of denoising method.

section, terms related to change of basis is elaborated to cover its importance and need in denoising.

In mathematics, specifically in linear algebra, basis is a set of vectors that can linearly combine to represent every vector in a given vector space [30]. In linear algebra, " a basis for a vector space of dimension n is a sequence of n vectors $[a1, ..., an]$ with the property that every vector in the space can be expressed uniquely as a linear combination of the basis vectors. Since it is often desirable to work with more than one basis for a vector space, it is of fundamental importance in linear algebra to be able to easily transform coordinate-wise representations of vectors and linear transformations taken with respect to one basis to their equivalent representations with respect to another basis. Such a transformation is called a change of basis. [30]" See Figure 4.2.

With small changes, the above theory can be used to formulate the use of change in basis in signal processing. In signal processing, instead of vectors, functions are represented by the combination of basis functions. The basis function is selected on their suitability to represent the original function and their application.

Note: The remote sensing images can also be considered as function of image brightness value w.r.t spatial location, as depicted in the following equation, x is spatial location and $Brts_x$ is brightness value at location x:

$$f(x) = Brts_x \tag{4.1}$$

Representing the function, say $f(x)$ with some other function, say $g(x)$ with some transformation $h(n)$ provides more control on function, which reflects hidden properties of the signal. See Figure 4.2, the properties of signal is acquired correlating the signal with basis, which more technically known as convolution.

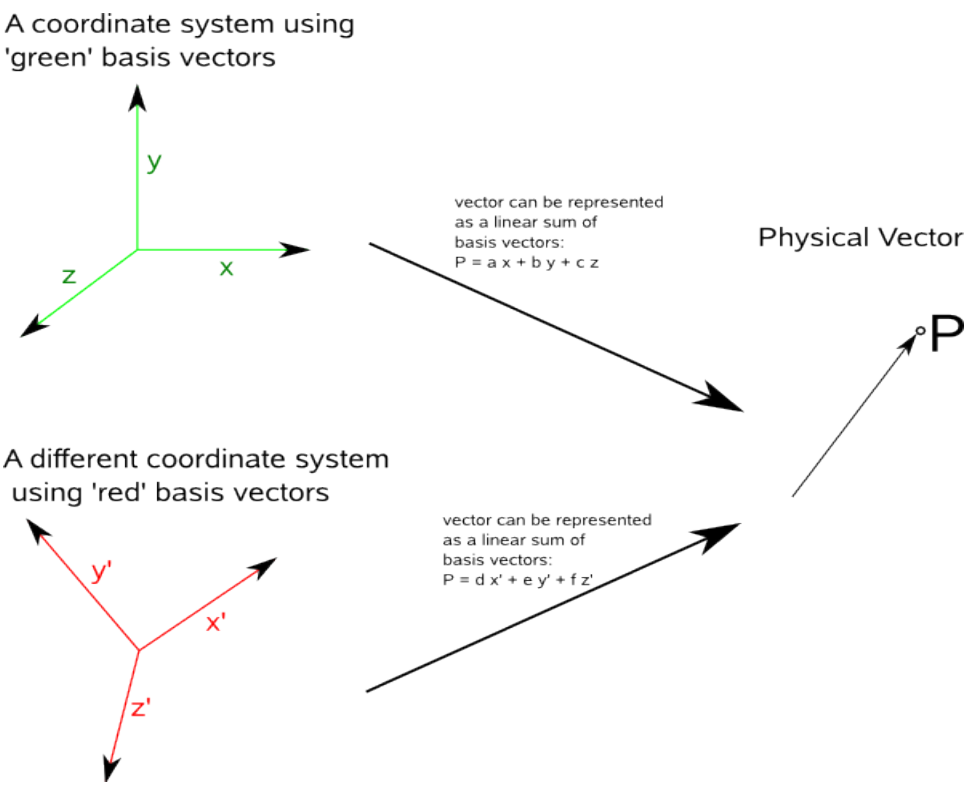

Figure 4.2: Shows the how the vector can be represented by different basis vectors. Source: www.dspguide.com

Without going into much detail, convolution can be understood as multiplication of basis and signal (in frequency domain).

$$x[n] \times h[n] = y[n] \tag{4.2}$$

After convolving the signal with basis, set of coefficients is obtained. These coefficients are the mathematical representation of the signal or function.

4.2.2 Preserving image information: The need to change basis.

In denoising, having mathematical coefficients instead of, mere DN values or magnitude of the signal, gives better advantage. As these coefficients facilitates better hold in terms of operations that can be applied to the signal. ***Removing***

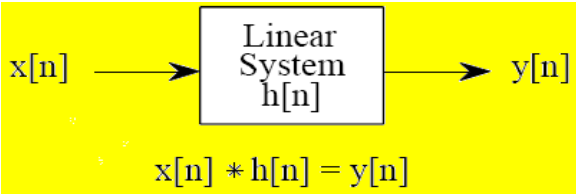

Figure 4.3: Shows the convolution operation Source: www.dspguide.com.

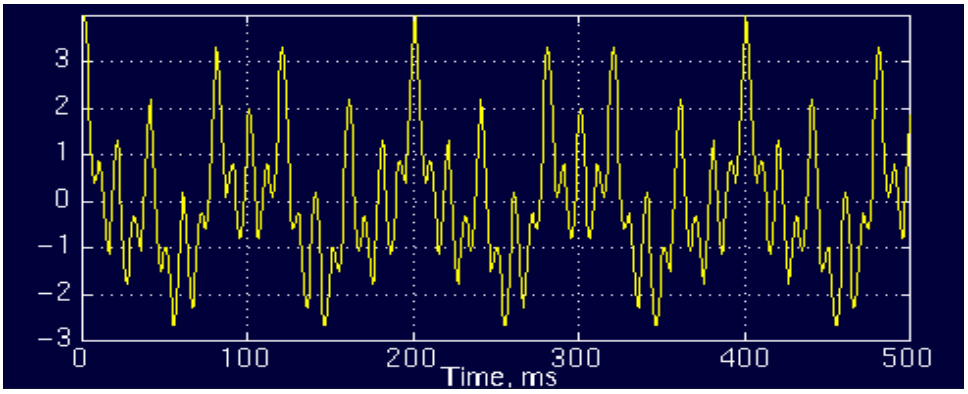

Figure 4.4: Shows the noisy signal. Source: (31)

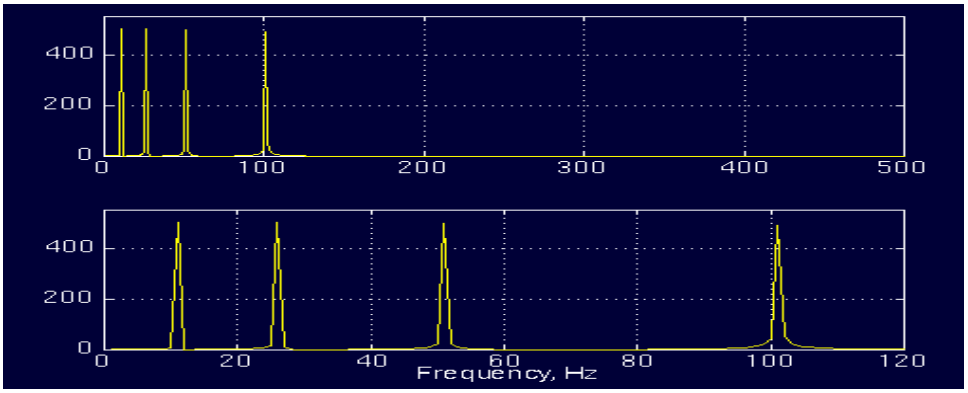

Figure 4.5: Shows frequency domain information Source. The upper and bottom part are the frequecy response of same the signal with the difference in zoom. Source: (31)

noise from the image is challenging task without this transformation. The challenge is to preserve the image information. Denoising method can penalize the edge information. It happens because edges and noise are both high frequency components. Just the DN values of image or amplitude of signal does not provide ample information to distinguish between edges and noise, which can be passed onto denoising function for better processing of edges.

This concept can be understood by looking at Figure 4.4 and 4.5. Figure 4.4 shows the noisy signal which has various frequency components and Figure 4.5 is the frequency domain representation of the same, which is obtain after a transformation (Fourier). The spikes in Figure 4.5 are the frequency present in signal shown in Figure 4.4. This information can not be depicted from noisy signal, which has not been transformed (Figure 4.4). ***Provided this information, an effective denoising method can be developed that take care of the information content of the signal.***

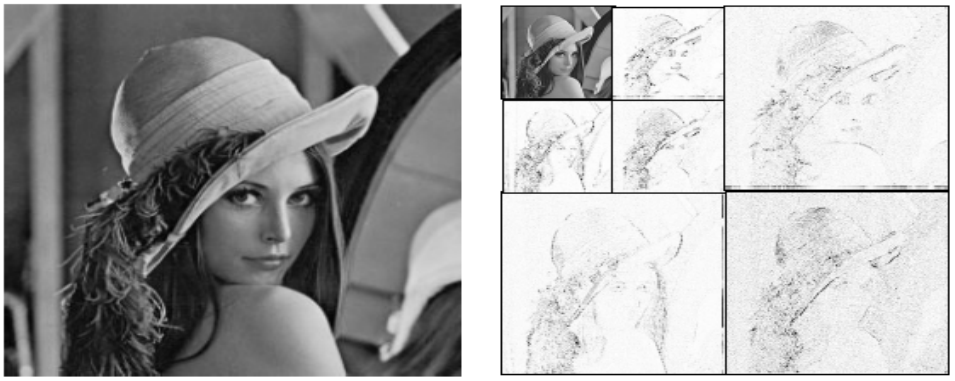

Figure 4.6: Shows the (a) Lena Image, (left) (b) DWT of Lena image, the dark pixels in the subbands denotes the coefficients with large magnitude. (2)

4.3 Importance of Wavelets

In the last section, importance of transformation in developing the denoising method is discussed. In this section importance of Wavelets in denoising is covered, skipping the basic transformation concepts of wavelets.

4.3.1 Eminent features of wavelet transform

1. **Edge detection property** The discrete wavelet transform (DWT) of an image provides the uncorrelated coefficients, which are not independent of each other. In Figure 4.6, it can be observed that coefficients have large magnitude (dark) when edge is encountered in image. And also, their spatial location is same in different subbands at same and adjacent scales [2]. This shows the edge detection capability of wavelet transform.

2. **Sparsity** Looking carefully at the magnitude of transformed coefficients, it can be seen that ***large number of coefficients are small in magnitude, while small number of coefficients are large in magnitude***. This property of wavelet coefficients is known as sparsity. As also seen in Figure 4.6, the coefficient's value is less (white) for smooth area of image.

3. **Multiresolution Analysis** Wavelet transform provides the mutiresolution images of the same image. This can be obtained by taking the DWT of the image at different levels, each time decomposing LL subband. Analyzing the image at different resolutions with subband information provides new information about the image. As this not only gives the option to see image at both coarse and fine resolution, but also simultaneously, allows establishing the coefficient relation with the scale. This $with - in$ scale relation provides new stories about the image under observation.

4. **Subband information** DWT of the image not only has the edge detection capability but also the local orientation of these edges can be described by the subbands i.e. $LH, HLandHH$ subbands. Looking at Figure 4.6, it

can be observed that with edge information, orientation of the edges is also visible. This can be seen by looking at the same feature in different subbands. The orientation of the coefficients is different. This happen because of the filtering techniques, which is different for each subband.

4.3.2 What about Fourier?

The Fourier transformation can also provide the edge information by providing the impulse in the frequency domain. But using Fourier transform in denoising does not provide enough information. The reason is Fourier is reversible process, that is, it allows to go back and forth between the original and transformed domain. However, only either of them is available to analyze at a given point of time. That is, no frequency information is available when in time domain, and no time information is available when in frequency domain [31]. In terms of images, the edge information can be extracted but its spatial location in the image can not be obtained. This can be illustrated clearly from Figure 4.4 and 4.5. In these two figures the presence of particular frequency is shown but its location information is lost.

In denoising, it is not only important to know the edges and its magnitude but also its spatial location, which plays an important role. Without knowing the spatial location of the edges, information content of the image may be penalized by the denoising method.

On the other hand, Wavelet transform facilitates with both the spatial and edge information together. This means while observing a specific coefficient,$coeff_x$, its spatial location and magnitude is known. Interesting fact is how it happens in wavelets? This is possible because of the following relation between image pixels and the coefficient

$$coeff_{i,j} = (i,j),(i-1,j),(i,j-1),(i-1,j-1) \tag{4.3}$$

The equation 4.3 shows, for $coeff_{i,j}$ pixels (shown in equation) will be used to derive its magnitude and what is that magnitude, it depends on the wavelet family and vanishing moment used.

This relationship between pixels and coefficients strengthen the transformation by providing both, the coefficient value and spatial location of pixels from which it is calculated. The coefficients in the wavelet transform forms the natural dyadic tree, which keep intact the relationship between pixels and coefficients up to higher levels of decomposition, see Figure 4.7.

This property of wavelet is known as ***spatially adaptive property***. Due to the above stated benefits, wavelet transform is selected as a domain in which denoising method have been applied in this research.

4.4 Noise Model

This section elaborates the noise model used in this research. As mentioned in *chapter 1*, selection of noise model is an important task. The denoising method depends mostly on the type of noise it handles.

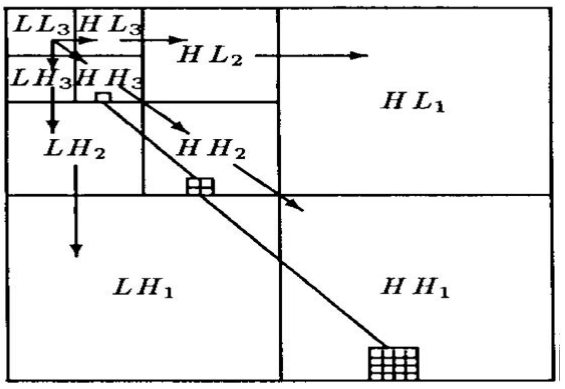

Figure 4.7: Shows the dyadic tree formation of wavelet transform.

As mentioned in chapter 1, quantization and thermal noise are the main source of random noise in image [36], which according to [35], can be modeled as Gaussian noise and also these are the main source of noise in images [36, 1]. Although other complicated noise model provides better results, but this is a subjective issue. A compromise between the complexity of the process, availability of information about the sensors and user's requirement, influence the choice of noise model. For this research work, ***additive noise model is most appropriate***, given the time constraint and restricted knowledge about the sensor.

To begin with the mathematics of noise model, let us denote the digital image with vector x, which is a clean image i.e. devoid of noise. If noise is denoted by η then the noisy version of the clean image x, according to additive noise model, can be expressed as:

$$y = x + \eta \tag{4.4}$$

The noise η is a random vector of random variables, while x, the clean image is an unknown or inaccessible. Here, y i.e. a contaminated image is the only thing accessible or known. However appropriate realization of the noise η can be made, which is based on the type of noise targeted.

Like noise model the noise type also plays a significant role in developing denoising method. If noise model on the one side suggests how the noise is added to the clean signal then noise type on the other hand provides the properties of the noise present.

Usually, it is assumed that the noise has zero mean ($E(\eta) = 0$), which means its covariance matrix is

$$Q = E[(\eta - E(\eta))(\eta - E(\eta)^T] = E(\eta\eta^T) \tag{4.5}$$

If the covariance matrix, Q , is diagnol, i.e. $E(\eta_l, \eta_k) = 0$ for $l \neq k$, the noise is correlated and can be called as *white* [2].

The Gaussian noise model has following probability density function:

$$p_\eta(\eta) = \frac{1}{(2\pi)^{\frac{n}{2}}\sqrt{det(Q)}} e^{-\frac{1}{2}\eta^T Q^{-1}\eta} \tag{4.6}$$

Finally, from all the above equations about noise, the concluding assumption is noise variables are independent, identically distributed (i.i.d). This is type of noise is known as *Additive White Gaussian Noise (AWGN)* [2]. And in this thesis the noise model and type is *AWGN*.

In the succeeding chapters, denoising method built upon the above assumption will be covered.

Chapter 5

Transformed Image Denoising: SURE-LET Shrinkage

"It is with logic that one proves; it is with intuition that one invents."— Henri Poincare

This chapter introduces the denoising technique, which is employed in this research work. The developed denoising method is based on SURE-LET approach in wavelet domain. Succeeding sections, discusses step by step methodology that is developed in this research work. In section 5.1, wavelet domain shrinkage concept is discussed. Section 5.2 discusses the SURE-LET technique and mathematics related to it. Section 5.3 and 5.4 discusses the implementation of SURE-LET approach on wavelet coefficients, which derived from spatial and spectral domain of the image. In section 5.4.3, new segmentation method, which is developed during this research work to reduce the number of spectral curves to be denoised, is explained.

5.1 Wavelet Shrinkage

Transforming the image space into wavelet domain and selecting the significant coefficients by a threshold technique is a popular approach for denoising. In its most basic form, *thresholding* of wavelet coefficients is performed in a orthogonal wavelet domain comparing each coefficient against a threshold T [2]. *If the coefficient is less than the threshold then it is set to zero otherwise it is retained as such or modified depending upon the type of thresholding used.* In denoising, pioneering work done by [7] had introduced this concept of shrinkage, which boils down the denoising problem to calculate the optimal T. And have also shown that in wavelet domain coefficients comprises natural sparsity property, which allows easy extraction of significant coefficient by some threshold. The central idea of [7] lies in the fact that various wavelet thresholding schemes for denoising have near optimal properties in the minimax sense, where minimax is an approach to derive an equation for calculating optimal threshold value.

The wavelet shrinkage approach can be understood and implemented in two simple steps:

1. **Determine Threshold :** In this step, optimal value for threshold is selected. [7] approach is to minimize the estimation of mean square error by stein unbiased risk estimate, known as *SureShrink*. By minimizing the *SureShrink* value optimal threshold can be selected. Certainly, many other techniqes exists to select the optimal T (Refer Chapter 2).

2. **Threshold type:** By threshold type it means operations performed on coefficients with threshold T. Two types of thresholding techniques are commonly used for denoising:

   (a) *Hard Thresholding* In this type, the coefficient is compared to the threshold value and if it is less than the threshold value then it is set to zero otherwise kept intact. This technique is also known as *Keep or Kill* [2]. Following equation explains the hard thresholding concept.

   $$T^{hard}(w) = \begin{cases} 0 & \text{,if} \quad |w| \leq T \\ w & \text{,if} \quad |w| > T \end{cases} \tag{5.1}$$

   (b) *Soft Thresholding* In this type, the coefficient is compared against the threshold value and if it is less than the threshold, it is set to zero otherwise the magnitude of the coefficient is shrink by an amount equal to the threshold value [2]. This technique is known as *Shrink or Kill*. Following equation explains the soft thresholding concept.

   $$T^{soft}(w) = \begin{cases} 0 & \text{,if} \quad |w| \leq T \\ (|w| - T) & \text{,if} \quad |w| > T \end{cases} \tag{5.2}$$

In this research work, *soft thresholding* type thresholding technique is applied. The justification lies in the disadvantage shown by hard thresholding method. Hard thresholding shows abrupt discontinuity, especially in case of high noise level, because of which abrupt artifacts in the reconstructed image can be viewed [2].

5.2 SURE-LET approach

In the last section, *soft and hard thresholding* is explained, which has important role in shrinking the noisy wavelet coefficient. Now, the important question is what should be the value of threshold T (Which is a first step in wavelet shrinkage approach)? In this section, method to select appropriate threshold value T is discussed.

In the last few decades, with advances in wavelet based techniques to calculate optimal threshold T have been parallarly developed. Broadly, these thresholding techniques work in two phases. In first phase, some method is applied to the wavelet coefficient to understand the trend of the signal. This helps in expressing the whole image with some mathematical equations. In the next phase, noise models are developed, which explains the nature of noise present. Integrating these two phases helps in forming a model that calculates optimal value T.

There are many wavelet based techniques available for calculating optimal threshold and careful selection of these methods is required. After rigorous literature survey, in this research work *Stein Unbiased Risk Estimate* (SURE) (Ref.: Chapter 2) is opted.

5.2.1 Risk estimation: SURE

In this part of the section, effort is made to first explain the mathematics behind SURE-LET approach. This understanding is important so as to enable one to apply SURE-LET as done in the current research work.

Suppose, given N noisy samples of some function f, such that:

$$y(i) = f(i) + z(i), i = 1, ..., N \tag{5.3}$$

Equation 5.3 refers to the additive noise model covered in chapter 4, section 4.4. This means no access to $f(i)$ (original image) and some assumptions for $z(i)$. The goal is to estimate the vector $f(i)$ with minimum mean square error (MSE), which means estimating some function $\hat{f}(i)$. Estimation of $\hat{f}(i)$ thus associate small *risk* R with it, such that:

$$R(\hat{f}, f) = \frac{1}{N} \cdot E||\hat{f} - f||_2^2 \tag{5.4}$$

Successful search of $\hat{f(i)}$ that has minimum $R(\hat{f}, f)$ is a solution to the denoising problem. For now onwards let us call a denoising problem a search of $\hat{f(i)}$ that has minimum $R(\hat{f}, f)$

Note: The main mathematics and equations of SURE-LET are taken from [3, 16, 7, 2, 14]

Above equation builds up the basics to understand SURE approach. Before proceeding to SURE-LET , let us first develop notation to understand MSE in subbands. The mean-square error (MSE), in space domain, of the whole image is equivalent to the sum of individual MSE of each subbands [3]. Mathematically, it can be expressed as:

$$\underbrace{\langle|\hat{x} - x|^2\rangle}_{MSE} = \sum_{j=0}^{J} \frac{N_j}{N} \underbrace{\langle|\hat{x}^j - x^j|^2\rangle}_{MSE^j} \tag{5.5}$$

As mentioned in Chapter 3 section 3.2, the aim of denoising method is to maximize the *PSNR* and minimize the *MSE*, which also is a measure of performance for any denoising method. Thus, to minimize the MSE expressed in (5.5), *SURE* estimates each $\hat{x}^j$ by a pointwise function θ [3].

$$(\hat{x_n^j})_{n\epsilon[1,N_j]} = (\theta^j(y_n^j))_{n\epsilon[1,N_j]} \tag{5.6}$$

The index j can be dropped from (5.6) since denoising function is applied on each individual subband. The aim is to build a function θ that minimizes, *MSE*:

$$MSE = \langle|\theta(y) - x|^2\rangle = \langle\theta(y)^2\rangle - 2\langle x\theta(y)\rangle + \langle x^2\rangle \tag{5.7}$$

Problem with (5.7) is its dependency upon x (Where x in this case is a clean image). It is required that explicit dependency on x should be removed, so that the function θ can be built without x. Careful observation of (5.7) shows that the additive term $\langle x^2 \rangle$ has no influence in minimization process, so this term can also be dropped from the estimation process. The next problematic term is, multiplicative term $\langle x\theta(y) \rangle$. If with some method this term can be removed from the equation then it is feasible to calculate the denoising function. In 1981 C Stein [32], proposed a theorem, which allows to overcome the problematic term $\langle x\theta(y) \rangle$. The theorem states:

Let θ be a differentiable function. Then the following random variable:

$$\epsilon = \langle \theta(y)^2 - 2y\theta(y) + 2\sigma^2\theta^{'}(y) \rangle + \langle x^2 \rangle$$

$$= \underbrace{\frac{1}{N}\Sigma_{n=1}^{N}(\theta^2(y_n) - 2y_n\theta(y_n) + 2\sigma^2\theta^{'}(y_n))}_{\tilde{\epsilon}} + \langle x^2 \rangle \tag{5.8}$$

is an unbiased estimator of the MSE.

As mentioned before the addititive term $\langle x^2 \rangle$ will not be used in the estimation. Thus remaining term $\tilde{\epsilon}$ is used to minimize the MSE and to choose θ. This typical formation of SURE ensures that if θ is so selcted that it minimizes the MSE then the function θ can also suppress the noisy coefficients.

5.2.2 Linear Expansion of Threshold: LET

In order, to make SURE approach computationally more efficient denoising method can be developed that *linearly* depends on some set of parameters, which can be determine by minimizing $\tilde{\epsilon}$ [3]. Developing this concept the denoising function θ can take the following form:

$$\theta(y) = \Sigma_{k=1}^{K} a_k \varphi_k(y) \tag{5.9}$$

Where, K is the number of parameters and φ_k is a basis which determines the shape of denoising function.

Introducing (5.9) into the MSE estimation given by (5.8) and performing the differentiations over the a_k, following relation can be obtained:

$$0 = \frac{1}{2}\frac{\partial \epsilon}{\partial a_k} = \langle \theta(y)\varphi_k(y) - y\varphi_k(y) + \sigma^2\varphi_k^{'}(y) \rangle \tag{5.10}$$

$$\Updownarrow$$

$$\Sigma_{l=1}^{K} \underbrace{\langle \varphi_k(y)\varphi_l(y) \rangle}_{M_{k,l}} a_l - \underbrace{\langle y\varphi_k(y) - \sigma^2\varphi_k^{'}(y) \rangle}_{c_k} = 0 \tag{5.11}$$

If equations (5.10) & (5.11) summarized in matrix form as $Ax = b$, where $x = [x1, x2, ..., x_k]^T$ and $b = [b1, b2, ..., b_k]^T$ are vectors of length $K \times 1$ and **M**

$= [M_{k,l}]$ is a matrix of size $K \times K$. Then this becomes a typical form of linear system that can be solved by:

$$x = M^{-1}b \tag{5.12}$$

The system as a linear system is very simple to implement and efficient in processing. Converting the denoising function θ into the linear system is known as ***Linear Expansion of Threshold*** (LET).

The only remaining question for solving the Equation 5.11 completely is the function θ. Certainly, there exist many functions that can be used in near optimal sense. According to [3], derivative of Gaussians (DOG) is an appropriate choice and can serve as a basis function φ_k, which determines the shape of denoising function. Also, [3] suggest to limit $k = 2$. This is because for $k > 2$ the results become quite similar and no significant improvement is observed. Thus, denoising function with DOG as basis and only two parameters $(k = 2)$ can take the following form:

$$\theta(y) = (a_1 + a_2 e^{-\frac{y^2}{12\sigma^2}})y \tag{5.13}$$

Equation 5.13 is a pointwise thresholding function and final denoising equation for SURE-LET based method. Using these simple yet powerful approach noisy images of the data set is denoised in wavelet domain.

5.3 Step-wise process to denoise the data set

In this section, operations involved in image denoising are discussed. Denoising image in transformed domain deals with: linear transformations, which consists $D - decomposition$ operation , $R - reconstruction$ operation and satisfies the identity property i.e. $RD = identity, I$. **In wavelet domain, D can be set of decimated or undecimated filters and if it is an orthogonal transformation then same filters can be used to reconstruct the image.**

This research work uses decimated filters for denoising. Main difference between decimated and undecimated filters lies in the processing done at each level of decomposition. For decimated filters, at every decomposition level size of the samples is made exactly half, which makes a natural dyadic tree structure. On the other hand undecimated filters, does not reduce the number of samples at every level, which means after every decomposition, number of samples remain same. These same samples at each level are repetitive samples, thus, does not contain any significant information, rather they are extra burden on processing unit.

Let us integrate operations $D\&R$ into Equation 5.9. As mentioned in the last section, LET approach allows to represent the denoising function as a set linear operations and have $Ax = b$ formation. In LET sense , operations $D\ and\ R$ can be characterized by matrices: $D = (d_{i,j})$ and $R = (r_{i,j})$, where $i, j_{\epsilon[1toN]\times[1toM]}$, which follows the perfect reconstruction property $RD = I$ [16].

The basic operations involved in denoising can be formed as a following sequence:

1. Apply operation D on noisy signal $y = x + b$ to obtain w noisy coefficients, such that $w = Dy$.

2. On the noisy coefficients w apply pointwise thresholding function θ, such as, $\Theta(w) = (\theta_{i(w_i)})$

3. Apply R on the denoised coefficients to reconstruct the image.

The whole denoising method can be summarized as the following function:

$$\hat{x} = F(y) = R\Theta(Dy) \tag{5.14}$$

SURE-LET equation for the above expression is:

$$F(y) = \Sigma_{k=1}^{K} a_k \underbrace{R\Theta_k(Dy)}_{F_k(y)} \tag{5.15}$$

5.4 Spatial and spectral denoising

In the last section, mathematics for denoising function Θ is developed and also its linear form as per SURE-LET is shown. In this section, the developed denoising function is shown to applied on data sets used in this research work. The whole denoising process is executed in two phases. In the first phase, denoising function Θ is applied on spatial domain i.e. on image space. Spatial domain denoising is a $2 - D$ signal denoising process. After spatially denosing the image, spectral domain denoising is done, which is the second phase. Spectral domain denoising is a $1 - D$ signal denoising process. This whole process can be understood as a $3 - D$ process in which x, y is the spatial domain and z is the spectral domain.

Mathematically, these processes are defined as:

$$x^{'} = R(\Theta_{spatial}(D(y))) \tag{5.16}$$

$$\hat{x} = R(\Theta_{spectral}(D(x^{'}))) \tag{5.17}$$

As mentioned, decomposition operation D decomposes the signal into subbands. Because of multiresolution analysis of wavelet domain, the decomposition process can be done at different level. These levels have different resolution of the same signal thus forming the natural dyadic tree structure. In order to incorporate the level information in decomposition operation D, parameter L is appended to it. Now, the decomposition operation D can be expressed as a function of two parameters, signal $(y)$and decomposition level (L):

$$D(y, L)$$

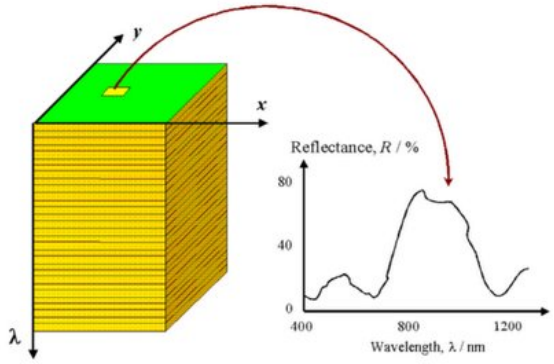

Figure 5.1: Shows the Hyperspectral cube and spectrum.

5.4.1 Spatial denoising pseudo code

In this part of the section, stepwise process to spatially denoise the image is shown.

(B = no. of bands)
begin (pseudo code 1)
For i = 1 To B

1. Take the band wise DWT of the image, i.e. apply operation D to get the coefficients of each band, y_i upto decomposition level L.

$$w_i = D(y_i, L) \tag{5.18}$$

2. $for\ each\ subband\ j\ \ and\ for\ each\ level\ l\ compute:$

   $\hat{X}_i = \Theta(w_{j,l})_{j \epsilon i}$

3. Take the IDWT of $\hat{X}$ to get the final denoised image, this is done by operation R:

   $\hat{x}_i = R(\hat{X}_i)$

end
end

5.4.2 Spectral denoising

Spectral domain denoising requires more bands that are contiguous and have narrow band width to produce spectral curve. For reference, Figure 1.2 is redrawn as Figure 5.1. The λ axis and the spectrum shown in the figure is the spectral domain. In order to remove the noise more efficiently this domain should also be used [4]. But as mentioned in Chapter 1 section 1.3.3, for fast processing number of curves should be reduced Ref. Chapter 1, section 1.3.3 for more detail). In this research work reduction in number of spectral curves is achieved by segmenting the image.

Though many efficient segmentation methods are available but in this research work new method for segmentation the image is designed. The reason to not to use any other method lies in the main objective. The objective is to reduce the number of curves so that lesser number of curves should be processed by denoising method. But certainly those curves, which did not pass through the denoising method has to be some how denoised. The idea is to select only one curve per segment for denoising and with the help of some relationship between pixels of segment, update the value of remaining pixels, which are not denoised by denoising method. **Our segmentation method may be less efficient in segmenting the image, but surely it establishes the relationship between the pixels within the segment and ensures the updating of values without actually passing all the pixels through denoising method.**

In the next part of the section, segmentation operation is discussed, then in the later part of the section it will be applied to spatially denoise images (as per equation 5.17).

5.4.3 My Segmentation approach

Denoising $C \times M \times N$ data set, where $M \times N$ = dimensions of image and C = number of bands requires computation time that grows exponentially with increase in image dimension. The segmentation can reduce the spectral curves to be denoised. Before going into the mathematical expression for this approach, let us take an example to understand out method.

Taking wavelet transform of an image using Symlets wavelet family with 1 vanishing moment($Sym1$) gives very interesting results. That result is a key of this approach.

$Let\ x\ be\ an\ 8 \times 8\ image =$

1	2	3	4	5	6	7	8
9	10	11	12	13	14	15	16
17	18	19	20	21	22	23	24
25	26	27	28	29	30	31	32
33	34	35	36	37	38	39	40
41	42	43	44	45	46	47	48
49	50	51	52	53	54	55	56
57	58	59	60	61	62	63	64

Apply the operation D on this image i.e. compute equation 5.18. This process will give the coefficients W

$W =$

11.0	15.0	19.0	23.0	-1.0	-1.0	-1.0	-1.0
43.0	47.0	51.0	55.0	-1.0	-1.0	-1.0	-1.0
75.0	79.0	83.0	87.0	-1.0	-1.0	-1.0	-1.0
107	111	115	119	-1.0	-1.0	-1.0	-1.0
-8.0	-8.0	-8.0	-8.0	-0.0	- 0.0	- 0.0	-0.0
-8.0	-8.0	-8.0	-8.0	-0.0	-0.0	-0.0	-0.0
-8.0	-8.0	-8.0	-8.0	-0.0	-0.0	-0.0	-0.0
-8.0	-8.0	-8.0	-8.0	-0.0	-0.0	-0.0	-0.0

In the above matrix of 8×8 size there are four subbands.

Subbands LL : dimension = 4×4 and index = Row :1 To 4 and columns : 1 To 4.

Subbands HL : dimension = 4×4 and index = Row :1 To 4 and columns : 5 To 8.

Subbands LH : dimension = 4×4 and index = Row :5 To 8 and columns : 1 To 4.

Subbands HH : dimension = 4×4 and index = Row :5 To 8 and columns : 5 To 8.

If we observe the property of these subbands then very interesting facts comes out. See the LL Subband coefficient $(1,1)$. It is 11. Now see the pixels $(1,1)$,$(1,2)$,$(2,1)$,$(2,2)$. They are 1 , 2 , 9 , 10, respectively in original image space. Add all of them and divide by 2, i.e. $22 \div 2$ = 11. Is that the coefficient value? The relation between all the coefficients of LL subband can be seen to follow the following equation:

$$Coef_{LL}(i,j) = \frac{[(i-1,j)+(i,j)+(i,j-1)+(i-1,j-1)]}{2} \tag{5.19}$$

Where, RHS representing the pixel location in original image space and LHS is the location of coefficient in wavelet domain. Now, check if LL subband satisfies the $equation$ (5.19) for all pixels or not. Fortunately, it is indeed satisfying.

Now, about other subband's coefficients, are they also mathematically linked with original image space? Yes, $equations$ can be represented as:

$$Coef_{HL}(i,j) = [(i-1,j)-(i,j)] + [(i,j-1)-(i-1,j-1)] \tag{5.20}$$

$$Coef_{LH}(i,j) = [(i-1,j-1)-(i-1,j)] + [(i,j-1)-(i,j)] \tag{5.21}$$

According to (5.20) the coefficient $(1,1)$ of HL subband should be $[(2-1) + (10-9)] \div 2 = 1$. Is it? Yes. Similarly according to (5.21) the coefficient $(1,1)$ of LH subband should be $[(9-1) + (10-2)] \div 2 = 8$.

The above example has set the basic idea of our approach. Let us now see the whole process more formally. The segmentation process can be done in three phases. Preceding part of this section explains these phases.

5.4.4 Phase One

Before we derive segments from wavelet coefficients it is important to define the small and large magnitude coefficients. The term small and large is relative thus, a reference is required. The reference is the $threshold$ T_m [7]. If a coefficient is less than T_m then it will be considered as small, otherwise large. Appropriate value of $threshold$ is very crucial. Since, the aim of this approach is to extract homogeneous regions or segments or objects, the threshold value T_m should be able to recognize the boundary of homogeneous area. After the extensive literature survey N Otsu [20] threshold selection method from Gray-Level Histograms, is selected to derive T_m for the method. Having the appropriate threshold to classify the wavelet subband coefficients, we can label the

subbands LH, HL and HH coefficients as significant and non-significant. Here significant coefficients corresponds to small magnitude coefficients with respect to $threshold\, T_m$. Let us define a coefficient in the subband S of the image as non-significant that exceeds a specific $threshold\, T_m$ and formulate the following two hypotheses: $H0$: "Coefficient is significant" and $H1$: "Coefficient is non-significant." mathematically as:

$$H0 : |\alpha| < T_m and H1 : |\alpha| > T_m \quad .....(5)$$

5.4.5 Phase Two

After labeling the coefficients as significant and non-significant in $phase$ 1, the next step is to map the significant coefficients onto the original image space to produce initial clusters. Before that, it is important to understand the chances of getting significant coefficients in a natural image. According to [6], in a wavelet domain, most of the subbands coefficients will be very small in magnitude and these small magnitude coefficients will be large in number, which can also be understood from a peaky heavy tailed distribution of wavelet coefficients. This ensures that we will surely get significant amount of small magnitude coefficients. $Figure$ 3 shows the distribution of wavelet coefficients.

To map coefficient onto the original image space we used $Equation4$ that gives us the exact spatial location of the corresponding image pixels. The natural tendency of wavelet coefficients ensures us that if the subbands LH, HL and HH coefficient is small in magnitude then the corresponding image pixels $Equation4$ will belong to the same homogeneous area. Recursively scanning the wavelet coefficients this way, we generate homogeneous regions or segments that that constituted four pixels, each. See $Figure2$ to see the dyadic relation between coefficients at coarse level of decomposition to finer level of decomposition.

5.4.6 Phase Three

The outcome of Phase two of our method is small segments which has size of four pixels. In order to merge these small segments we will further decompose the subbands LH, HL and HH. This approach is contrary to the idea of decomposing only LL subband. The decomposition of subbands LH, HL and HH will give us the new sub-subands, which will corresponds to 4×4 pixels in the original image space. Again, the significant sub-subands coefficients will be extracted using $threshold\ T_m$. Mapping the sub-subands' coefficients from its corresponding subband and finally to image space we can have automatic merging of the small segments that were produced in Phase 2.

To understand this concept more clearly let us take an example. Suppose we have a natural image of size 8×8 and the image has four segments. The spatial location of these segments is: Segment 1 is from row $(1 : 4)$ and column $(1 : 4)$, Segment 2 is from row $(1 : 4)$ and column $(5 : 8)$,Segment 3 is from row $(5 : 8)$ and column $(1 : 4)$ and Segment 4 is from row $(5 : 8)$ and column $(5 : 8)$. Now, taking the DWT(Decomposition Level 1) of this image will

give us four subbands LH, HL and HH. The LL subband will be a coarse representation of the image. We'll not utilize this LL subbands. Looking at the other subbands LH, HL and HH we found that their coefficients are representing the horizontal, vertical and diagonal difference of the corresponding four $(Equation4)$ pixels of original image space. Now, if the value of any coefficient, say at (i, j) w.r.t $thresholdT_m$ then it can be infer that the corresponding four image pixels $(Equation4)$ will belong to same segments. Processing this way we can generate 2×2 size segments. Now again taking the DWT, this time of the subbands LH, HL and HH (Decomposition Level 1) will give us the four subsubands. The small value of the coefficients value with respect to $thresholdT_m$ will give us the segments of size 4×4. This is equivalent to our original image space. Ideally, processing should stop here for this example. But because the approach is unsupervised, the decomposition has to take place up to higher levels also. Thanks to the singularity measure property of wavelet transform, unnecessary higher level decomposition does not harm the results.

5.4.7 Spectral denoising pseudo code

In this part of the section, pseudo code to denoise image in spectral domain is present. The method is similar to the spatial domain denoising code except the two differences. First, denosing signal is $1 - D$ rather than $2 - D$ and second, segmentation operation is involved before applying function θ to the noisy coefficients.

begin (pseudo code 2)

1. Take DWT of the selected band, i.e. apply operation D to get the coefficients of any Band, y_i up to decomposition level 1. **(For segmentation purpose only one band is required, because other bands can be automatically segmented. For HySI data set Band number 50 is selected as it is the less noisy comparative to others. For synthetic data set any band can be selected.)**

$$w_{50} = D(y_{50}, 1) \tag{5.22}$$

2. Apply the segmentation operation to segment the selected band.
   $SegmentedImage = Seg(w_50)$

end

After segmented the image denoising process can begin which only denoise representative spectral curve per pixel.

begin (pseudo code 3)
For i = 1 To N, Where N is total number of pixels in a band.

1. Take the band wise DWT of the signal, i.e. apply operation D to get the coefficients of spectral curve, y_i up to decomposition level L.

$$w_i = D(y_i, L) \tag{5.23}$$

2. $for\ each\ subband\ j\ \ and\ for\ each\ level\ l\ check\ and\ compute:$

   If (w_i) is a representative pixel of a segment, Then

   $\hat{X}_i = \Theta(w_{j,l})_{j\epsilon i}$

   Else

   Update the pixel value using equation 5.19 To 5.21

   End

3. Take the IDWT of $\hat{X}$ to get the final denoised signal, this is done by operation R:

   $\hat{x_i} = R(\hat{X}_i)$

end
end

Chapter 6

Results

This chapter presents the results from the method discussed in chapter 5 on three data sets used in this research work. The chapter is outlined in such a way that each section is an answer to research question mentioned in chapter 1. Answer to these questions is given by the results obtained.

6.1 What is the suitable wavelet family, support size and vanishing moment for the given wavelet?

According to [2, 3, 16], for denoising purpose Sym wavelet family with higher vanishing moment is best suited. The best way to verify the theory is to decompose and reconstruct the image using different wavelet families. This operation gives us two types of images. One is original image and second is reconstructed image. Because both resultant and original image is available computation of MSE and PSNR is possible, which is a reliable and easy measure for checking the accuracy of any process.

As mentioned in chapter 3, some bands of HySI sensor is visually more clean than others, like Band $45 - 55$. Inspecting decomposition and reconstruction is easier on clean band, therefore one of the band from the given range should be selected, say Band50.

Band 50 of HySI sensor is first decomposed using Symlet and Daubechies wavelet family with vanishing moment $1 - 8$ and then reconstructed using the same filter. Table 6.1 shows the results obtained from this process.

6.2 What is the most suitable decomposition level for the given problem?

In this section, results representing the best decomposition level are present. According to [33], measuring the entropy after each decomposition divulge if decomposition is of interest or not. Using the method of [33], it is found that for all three data set: HySI (256×256), synthetic image (256×256) and OCM (256×256) images decomposition up to fourth level is best suited. The entropy values up to level five is shown in Figure 6.1. The decomposition should be

Table 6.1: Shows the MSE and PSNR for Band50 HySI image reconstructed using DB and Sym wavelet family.

Wavelet Family	MSE	PSNR
DB1	5.13 e^{-024}	295.90
Sym1	4.30 e^{-026}	301.79
DB2	3.02 e^{-018}	218.92
Sym2	1.21 e^{-020}	247.29
DB3	1.36 e^{-017}	213.70
Sym3	1.99 e^{-018}	225.24
DB4	9.13 e^{-020}	231.97
Sym4	8.13 e^{-021}	249.02
DB5	4.06 e^{-015}	203.20
Sym5	9.62 e^{-022}	258.29
DB6	5.26 e^{-014}	191.25
Sym6	6.98 e^{-023}	267.31
DB7	3.30 e^{-011}	162.32
Sym7	2.90 e^{-025}	292.02
DB8	6.30 e^{-009}	140.97
Sym8	3.65 e^{-026}	307.10
DB9	7.58 e^{-008}	131.24
Sym9	5.39 e^{-026}	306.26

stopped when entropy value reaches to 0. And value before 0 is taken as best decomposition level.

6.3 What technique should be adopted for reducing the number of spectral curves?

In this research work, number of spectral curves is reduced by segmenting the image. Image segmentation is a technique to partition the image into multiple segments that are homogeneous in nature [24].

Table 6.2 shows the results of segmentation approach developed in this research work. The segmentation approach is experimented for different types of images, as shown, so as to check the approach under high variability in terms of scene complexity. Also, the quantitative results in terms of time taken by the method for each image are shown in Table 6.3.

The main aim of the segmentation is to reduce the number of spectral curves to be denoising. From the results it is observed that number of spectral curves reduced to 12584, which was originally 65536. Percentage decrease over this is 80%. In the succeeding sections, results of denoisng are based on both spatial and spectral based denoising with segmentation method included.

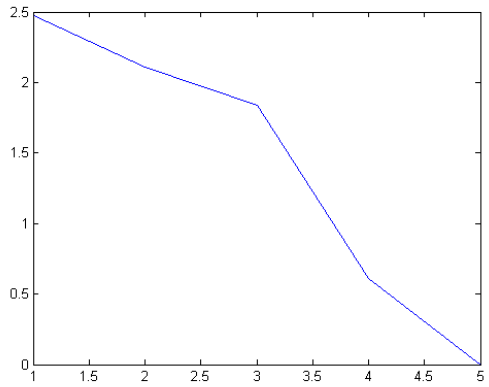

Figure 6.1: Shows the entropy value up to fifth decomposition level. At every level of decomposition the signal looses its detail and at fifth it reaches to zero. Hence, fourth level is best suited.

6.4 How to link the pixels in segments to update their values?

In Chapter 5, section 5.4 the new segmentation that is developed during this research work is explained. It also explains Equation 5.19, 5.20 and 5.21, which are the equation that establishes the relationship between each pixel with in the segment. These equations were used to update the pixel values within the segment, after denoising. The 12584 curves are denoised using function θ and remaining 52952 curves are denoised by linking using the mentioned equations.

6.5 Which validation technique is suitable when no reference image and no sensor parameters are known?

After an intensive literature survey and rigorous discussion with supervisors following validation measures are adopted in this work:

1. **Statistical method**
   (a) Standard Deviation within the smooth area (reservior in HySI).
   (b) Standard Deviation at the edge of class
2. Simulated image
   (a) MSE
   (b) PSNR
3. Non-Strip line value

Results of the above validation measures are shown in section 6.7.

Table 6.2: Shows the results of segmentation approach

Name and size	Original Image	Segmented Image
(a) Lena 512×512		
(b) Coco 256×256		
(c) Cameraman 256×256		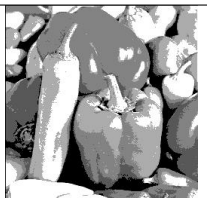
(d) Peppers 256×256		
(e) HySI Image 256×256	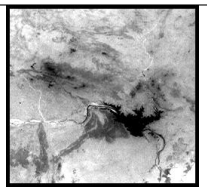	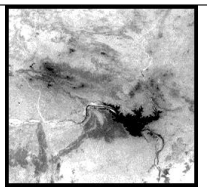

6.6 How to validate the noise level estimator?

To validate the noise level estimator a synthetic image is created. In the synthetic image noise is added whose level is known. Then the noisy image is processed through noise level estimator. The results can be matched to the known value of noise. Table 6.4 shows the results of the processing. Noise is estimated for different levels.

6.7 Results of denoising

This section presents the results obtain from the denoising method developed. The section is further divided in sub sections. Each sub section presents the result of one particular data set and comparison with two state-of-the-art tech-

Table 6.3: Shows the computation results of segmentation approach

Image Name	Size	Time	Wavelet Family
Lena	512×512	1.001418 sec	Sym8
Coco	256×256	0.257320 sec	Sym8
Cameraman	256×256	0.237724 sec	Sym8
Peppers	256×256	0.245363 sec	Sym8
Statellite Image	256×256	0.217789 sec	Sym8

Table 6.4: Shows the results of noise level estimator

Noise level added	Noise level estimated
5 db	5.05
10 db	9.85
15 db	15.15
20 db	19.98
30 db	29.20
60 db	59.42

niques. Beginning with HySI images section ends with OCM image result. The results are compared for three bands of HySI and simulated data set. The HySI bands are selected based on the noise level present and to cover the spectrum range. The simulated image was created to exactly map with HySI wavelengths, thus, for simulated image also same wavelength is used for comparison as that of HySI. For OCM data set one band is shown. Before proceeding to individual data set, the wavelength for HySI and simulated image is shown.

Full Wave Half Maximum wavelengths

1. **HySI Band 15** $547.4nm$ – **Simulated Band 15** $549.0nm$

2. **HySI Band 63** $947.7nm$ – **Simulated Band 63** $948.4nm$

3. **HySI Band 64** $956.0nm$ – **Simulated Bandd 64** $956.4nm$

6.7.1 HySI images

As mentioned in Chapter 3, HySI sensor has 64 contiguous bands. Because of space limitation in this part of the section results of three bands are shown. Table 6.5 depicts the results of denoising method applied on HySI images.

Standard deviation of the reservoir is measured at two main locations. One within the reservoir i.e. from the smooth part of the reservoir & the second is at the edges of reservoir.

Visually, improvement in results is seen to improve. Table 6.6-6.8, shows the visual results of three bands.

Table 6.5: Shows the two tables UP and DOWN. UP table shows the standard deviation of reservoir and the DOWN table shows the standard deviation at the edge of reservoir.

Band Number	Noisy Band	SURE-LET	ProbShrink	BLS-GSM
Band 15	11.89	**9.46**	10.01	10.65
Band 25	14.89	**13.19**	14.45	14.17
Band 63	3.60	**1.64**	2.08	2.48
Band 64	3.071	**0.91**	1.34	1.66
Band Number	**Noisy Band**	**SURE-LET**	**ProbShrink**	**BLS-GSM**
Band 15	23.17	21.67	21.18	**22.46**
Band 25	49.07	48.41	48.11	**48.78**
Band 63	33.49	28.46	27.34	**29.85**
Band 64	27.63	**23.40**	23.20	23.32

Table 6.6: Shows the results of denoising method on Band 63 of HySI

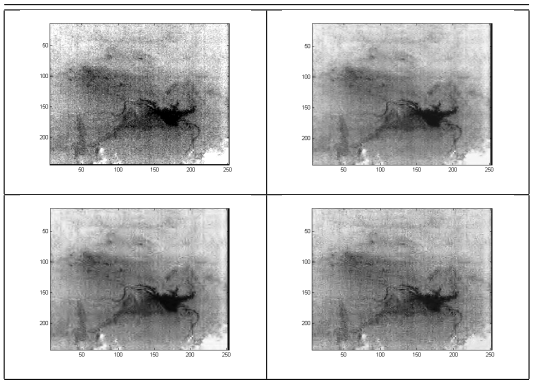

6.7.2 Simulated Image results

In this part of the section, results of denoising method on simulated image are presented. The simulated image is shown in Table 6.9(Left), each quad is presents one class. The noisy image with two noise level is shown in Table 6.9 (Middle and Right) (though simulated image is tested for 5 db, 10 db, 15 db and 60 db noise level but only two noisy images are shown because of space constraint). Quantitative results in terms of MSE and PSNR are shown in, Table 6.10, 6.11, and in 6.12. And finally, denoised image using SURE-LET, ProbShrink and BLS-GSM methods have shown in Figure 6.13.

6.7.3 OCM images

Denoising method applied to OCM 8 images (8 Bands). But results obtained are not satisfactory. SURE-LET method completely failed to remove strips from the images. Visual interpretation shows that strips exist as it was before destriping. Even other two methods, ProbShrink and BLS-GSM has same results, they are unable to remove strips from the images. It is clearly visible from Table 6.14.

Table 6.7: Shows the results of denoising method on Band 64 of HySI

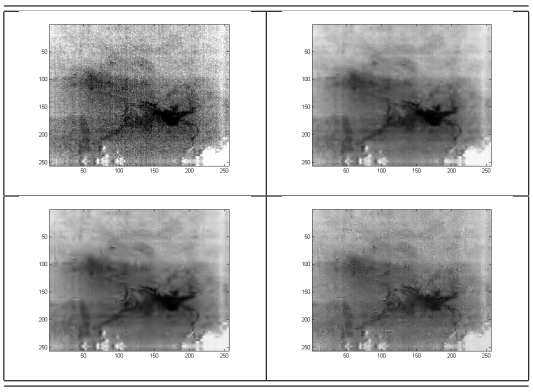

Table 6.8: Shows the results of denoising method on Band 15 of HySI

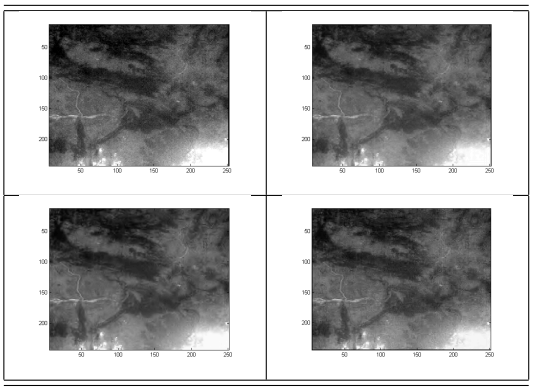

Table 6.9: Shows the (left) Simulated image Band 10 (middle) Noisy version with 10 db noise (right) Noisy version with 60 db noise.

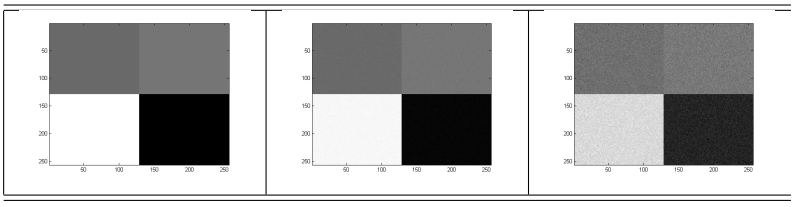

Table 6.10: Shows the improvement in MSE with SURE-LET, ProbShrink and BLS-GSM UP. Shows the improvement in PSNR with SURE-LET, ProbShrink and BLS-GSM. DOWN

Noise Level	**MSE input**	**SURE-LET**	**ProbShrink**	**BLS-GSM**
5 DB	24.9914	**2.4786**	3.4133	5.9944
10 DB	99.9658	**8.7832**	13.3852	25.8899
15 DB	224.9230	**18.1686**	25.9967	61.6609
20 DB	399.8630	**29.8070**	43.7826	113.5828
25 DB	624.7860	**43.1737**	61.9137	181.2134
30 DB	899.6919	**57.9476**	82.0810	264.5362
60 DB	3.5988e+003	**170.5669**	241.2196	1.0986e+003
Noise Level	**PSNR input**	**SURE-LET**	**ProbShrink**	**BLS-GSM**
5 DB	34.1529	**44.1888**	42.7991	40.3533
10 DB	28.1323	**38.6943**	36.8645	33.9995
15 DB	24.6105	**35.5376**	33.9816	30.2307
20 DB	22.1117	**33.3876**	31.7178	27.5777
25 DB	20.1735	**31.7786**	30.2129	25.5489
30 DB	18.5899	**30.5005**	28.9884	23.9060
60 DB	12.5693	**25.8119**	24.3067	17.7225

Table 6.11: Shows the MSE for all the 64 bands (and 1 class) (Starting from left) MSE input at 10 db noise level, MSE SURE-LET at 10 db noise level, MSE ProbShrink at 10 db noise level, MSE BLS-GSM at 10 db noise level

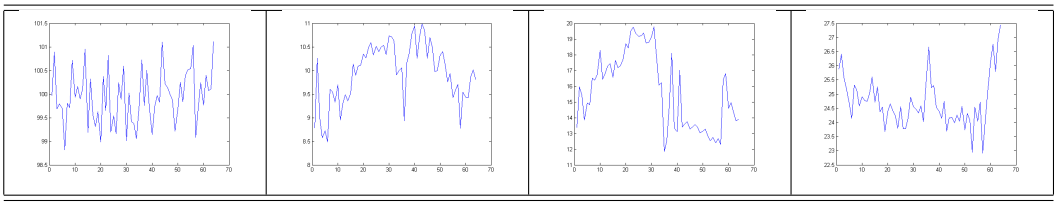

Table 6.12: Shows the PSNR for all the 64 bands (and 1 class) (From left) PSNR input at 10 db noise level, PSNR SURE-LET at 10 db noise level, PSNR ProbShrink at 10 db noise level, PSNR BLS-GSM at 10 db noise level

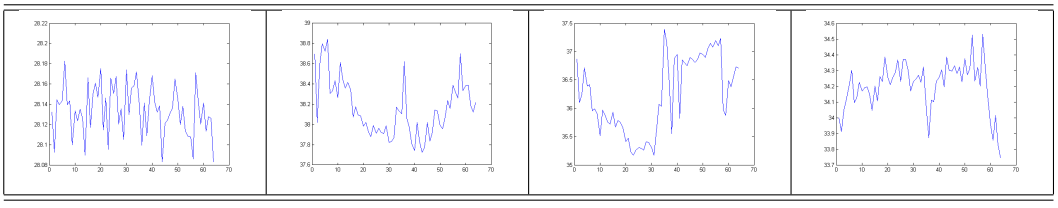

Table 6.13: Shows the denoised image (From left) Noisy image at 60 db noise level, Denoised using SURE-LET method, Denoised using ProbShrink method, Denoised using BLS-GSM method

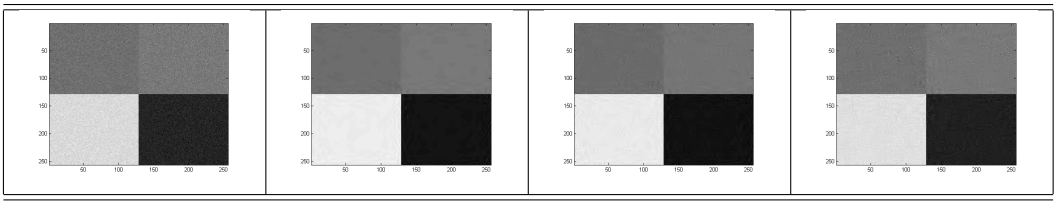

Table 6.14: Shows (From left) the noisy OCM Band 1 image. Strips in the image are the systematic error of the sensor, Denoised version by SURE-LET, Denoised version by Prob-Shrink,Denoised version by BLS-GSM

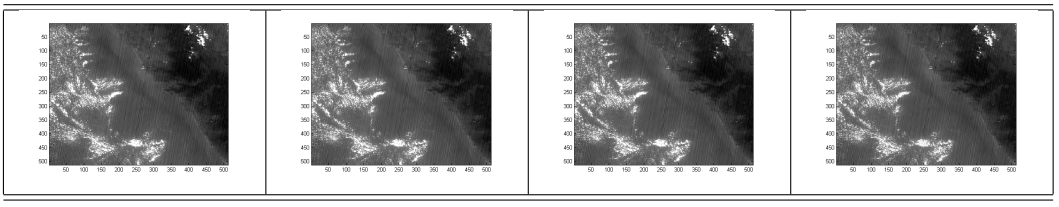

Chapter 7

Discussion

This chapter discusses the results presented in chapter 6 on three data sets used in this research work. The chapter is outlined in such a way that each section discusses the results of research question presented in chapter 6. Answers to these questions justify the choice of methodology.

7.1 What is the suitable wavelet family, support size and vanishing moment for the given wavelet?

This question refer to the operation D defined in Chapter 5, section 5.3. Equation 5.18 shows that the image is decomposed up to level L for wavelet transformation. It is important to consider the wavelet family that has to be used because different wavelet families convolve differently with signal and thus, resulting into different set of coefficients that has different properties [5]. Not all of these properties are suitable to be used for a particular application [2, 16, 7].

7.1.1 Symlet wavelet family

According to [14, 2, 3, 16], symlet wavelet family, which has compact support and near symmetric shape is best suited to denoising problem as compare to Daubechies wavelet family (DB) or other orthogonal wavelet families. The reason lies in the sparse representation and the structure of symlet wavelets, which meet the following requirement of denoising.

7.1.2 Required properties of coefficient for denoising

It is important to review the properties of coefficients required for denoising as it helps in selecting best family. First, wavelet coefficients should be sparse representation of the signal. Second, there should be no effect on visual quality of reconstructed image [2, 3].

1. **Sparsity** For sparsity convolving wavelet filter should produce, as many as possible, coefficients W_i that are near to zero. Two factors determine this result :

(a) Regularity of the analyzed signal at that instance. But it can not be controlled as it is signal characteristic not the filter's.

(b) Symmetry in filter's shape, which is controlled by vanishing moment (N_v) and the support size K of the filter [2]. The vanishing moment (N_v) should be as large as possible and support size K as small as possible [5]. It is because of the fact that polynomial component of the signal having degree less than (N_v) lies in a complementary scaling space, which yields to sparsity [5, 2].

2. Visual quality: Visual quality refer to less artifacts and blocks in reconstructed image. Smoothness in filter's shape ensure that the reconstructed image is visually

To meet these requirements, the shape of the filter should be smooth and convolving wavelet filter should be symmetric (near). Symlet wavelet family has more symmetry in shape as compare to DB, see Table 7.1. As mentioned, symmetry in shape ensures sparsity of coefficients [2, 5]. Symlet wavelets are also smooth in shape as compare to DB, see Table 7.1. Smoothness ensures less artifacts in reconstructed image, and hence, do not deteriorate the visual quality of it. Further, with increase in vanishing moment the symmetry and smoothness of wavelet filter improves [2], see Table 7.1. It is therefore recommended to use higher vanishing moment Symlet wavelet family for denoising [2, 5, 7].

The point can be justified by observing the results in Table 6.1 (Chapter 6). The results are consistent with theory. Though Sym1 and DB1 has better MSE and PSNR but image reconstructed using these filters has blocks and artifacts which are quite visible, which is not the case for the image reconstructed using higher vanishing moment filter, see Table 7.1.

Table 7.1: 1st row shows the reconstructed image using sym8 and DB1 family. 2^end row shows DB and Sym wavelet family filter's output

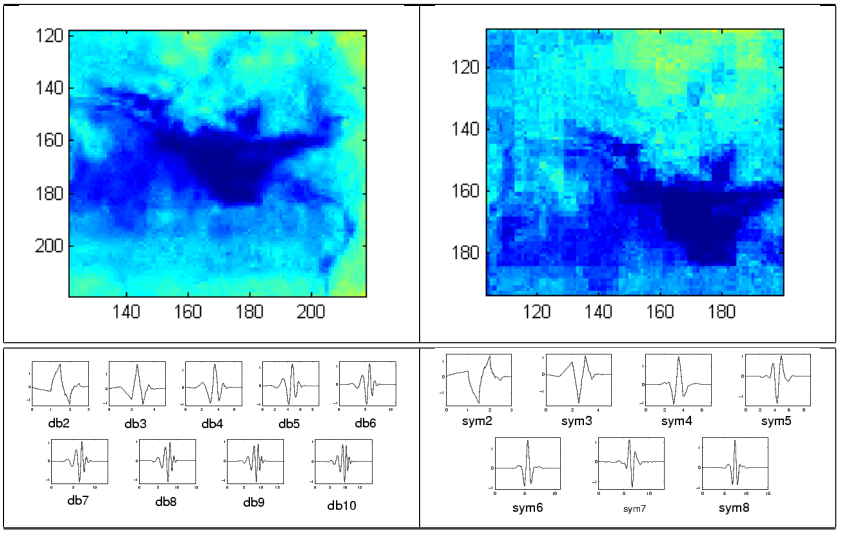

7.2 What is the most suitable decomposition level for the given problem?

In this section, answer to the problem of decomposition level is discussed. While decomposing a signal, level of decomposition (Ref: Chapter 5, equation 5.18.) has to be calculated.

7.2.1 Why it stopped at Level 4!!

From the literature surveyed, it is found that measuring the entropy after each decomposition divulge if decomposition is of interest or not [33]. According to [33], if the entropy of approximate subband i.e. LL is less than the entropy of the original signal's entropy and greater than 0 , then further decomposition should be done. Following are the basic steps to implement the method of [33]:

1. Compute the entropy of the original signal X.
2. Decompose the signal X up to level 1.
3. Compute the entropy of the approximate and detailed subbands.

   IF entropy of the detailed and approximate subbands $<$ entropy of the original signal and $>$ 0 Then

   Decompose further and repeat step 3

   ELSE

   Store the current decomposition level L, which is a result and Exit.

   END

Shannon Entropy basically measures the information content of the signal or any vector. In case of wavelet transform, entropy measures the roughness or regularities or more generally, edges of the signal. Because of the multiresolution analysis of the wavelet, at every level of decomposition signal looses its detail. The details are basically stored in LH, HL, HH subbands and approximation signal stored in LL subband. This is an iterative process until decomposition is not stopped.

The concept is illustrated in Figure 7.1, where at each level the detail of the signal is shown to be lost. Thus, measuring entropy means measuring the edge information. Interesting point is when there is no more edge information remain in the approximate signal, ideally, that is the best level to stop further decomposition, because beyond that nothing will be there for LH, HL, HH subbands. When the value of entropy reaches to zero, ideally that is the point when no significant edge remains in the approximate subband and further decomposition is not significant.

For data sets used in this research work level 4 decomposition was the point when Entropy reached to zero. This is a justification for decomposing the images up to level 4 only and answers to research question 2.

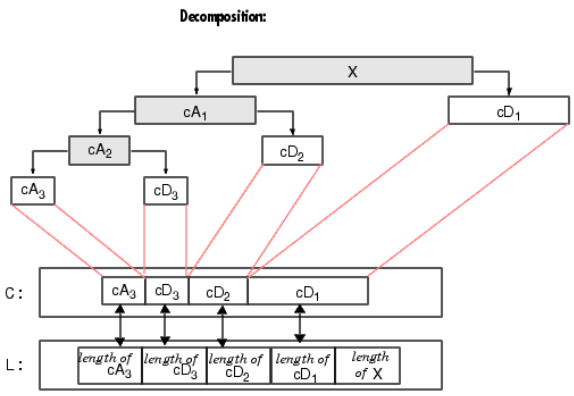

Figure 7.1: Shows the wavelet decomposition steps. At every level of decomposition the signal looses its detail.

7.3 What is the technical applicability of SURE-LET for hyperspectral data?

As mentioned in chapter 2 that the SURE-LET [3, 16] algorithm was developed for medical image denoising by Biomedical Imaging Group, Switzerland (BIG). There are lot of differences between the acquisition system of remote sensing and medical imaging. This questioned was posed in order to understand the technical limitations of SURE-LET algorithm for hyperspectral remote sensing data.

After analyzing the algorithm it is found that SURE-LET algorithm denoise the subbands of the image and then reconstruct the clean subbands to construct the denoised image [16]. The only thing which influences the result is the level of decomposition, which control the number of subbands [5]. It make the denoising method independent to acquisition type, as long as the noise is $AWGN$ [3]. Hence, SURE-LET algorithm can work equally well for remote sensing data and in this case for Hyperspectral data.

7.4 What technique should be adopted for reducing the number of spectral curves?

In this research work, developed segmentation technique uses the gray levels of the image. The reason is the resolution of images used in the research work. As mentioned in Chapter 3, the HySI sensor's data is acquired at $505m$ and OCM sensor's data at $360m$, which is a coarse resolution. In coarse resolution the terms like shape, size and texture can not be used because each pixel contains many classes with in it.

The homogeneous area of the segmented image mainly contains segments that can also be called gray level segments because they are formed using gray levels of the image [20]. Further, the gray levels of image is formed by quantization process [20]. On each gray level the effect of noise is same i.e. within

1 LSB the noise has equal effect on signal [36]. Thus, on each segment also the effect of noise is same, which allows denoising only one spectral curve per segment. And from this denoised spectral curve values of other spectral curves can be updated. The process, thus, does not denoise all the spectral curves and hence saves the processing time.

This can be justified from the results shown in chapter 6. It is shown that with the developed segmentation approach the number of curves reduced to 12584. This is a significant reduction in number of curves as denoising function is executed for 80% less spectral curves. Hence, takes less time to denoise the image.

The 80% reduction in spectral curves is achieved because of the following two reasons:

1. Linking of pixels: As mentioned in chapter 5 that other segmentation methods could achieve the better results. But the linking of pixels enables us to denoise only one curve per segment.

2. Merging: Decomposing subbands other then LL subband strengthen the segmentation method, as it enabled the merging of the small segments.

7.5 How to link the pixels in segments to update their values?

Symlet wavelet with one vanishing moment has interesting property that it is capable of generating natural segments of image in each subband [2] and enable to develop the equation that can map each coefficient to image directly [34]). Further if the segments detail subbands i.e. LL, HL, LH are decomposed, which is contrary to the practice of decomposing only LL subband, then small segments produced in phase 1 (Ref. Chapter 5) can be merged. This can also be justified by Equations 5.19, 5.20 and 5.21 (Chapter 5) that establishes the relationship between pixels and coefficients. These equations use the natural dyadic tree structure of the wavelet to map the wavelet coefficients to image pixels.

The important point is usually wavelet based methods suffers with alignment problem. Due to the shift variant nature of the wavelet decomposition, subbands at each level miss aligned from there position. This disturbs the dyadic structure of the wavelet. If subbands are misaligned then Equations 5.19-5.21 can not work. But higher level decomposition enable the segmentation process to merge the segments, which is an important in segmentation [20]. To overcome this problem the segmentation method is developed in such a way that only first level of decomposition is required. This is achieved by decomposing detail subbands i.e. LL, HL, LH [34]. Hence, question of alignment does not arise. Otherwise, to align the subbands special filters has to be employed [3, 16].

7.6 Is wavelet family used for denoising and segmentation are same?

As mentioned in section 7.1, best basis selection depends upon the application. In section 7.1 it was said that for denoising purpose smooth wavelet with higher vanishing moment and small support size performs better. But for segmentation process, developed in [34], wavelet function with less vanishing moment is best suited. Does that mean conclusion given in section 6.1 is wrong? No and the reason is as follows:

1. **Objective:** The segmentation process work only at first level of decomposition [34] and decomposes LH, HL, HH subbands not the LL subband. This is because segmentation process works with the detail information of the image not with the approximate information and LH, HL, HH subbands have detail information. This require crumple wavelet filter. From Table 7.1, it can be seen that low vanishing moment are fullfil this requirement.

2. **No reconstruction :** Unlike denoising process, segmentation process does not require to reconstruct the decomposed image, it directly map the subband coefficient to the image domain [34]. Thus, wavelet filters which are not smooth in nature can be used for segmentation without concerning about image visual quality.

With above justification, the wavelet used for segmentation process is Symlet with one vanishing moment because of its special properties mentioned in [34].

7.7 Which validation technique is suitable when no reference image and no sensor parameters are known?

Due to the reasons mentioned in Chapter 1 and Chapter 3 sensor parameters are not used in this research work for denoising the images. This force to think upon the effective validation technique that can verify and quantify the research work.

After an intensive literature survey and rigorous discussion with supervisors following validation measures are adopted in this work:

1. **Statistical method**

   (a) **Standard Deviation within the smooth area (reservior):** For HySI imageries standard deviation of the smooth area can quantify the denoising method's performance. HySI scene used in this work has reservoir (Hirakud Dam), which is the largest dam of India. Meauring the Standard deviation of reservoir can be taken as a measure of noise.

(b) **Standard Deviation at the edge of class :** The standard deviation at the edge mainly measure the performance of denoising function in terms of preserving edges. The standard deviation of the reservoir can quantify the edge preserving performance of the denoising method.

2. Simulated image: As mentioned in chapter 3, simulated image is used to quantify the results of denoising method. Noise of known standard deviation is added to the simulated image that allows quantifying the performance of denoising method by following two strong measures:

   (a) MSE: As per literature surveyed, mean square error is robust measure to quantify the performance of any method. The MSE of the denoised image should be less than the noisy version.

   (b) PSNR: Like MSE, PSNR is another robust measure to quantify the performance of any method. The PSNR of the denoised image should be grater than the noisy version.

3. **Non-Strip line value**: To quantify the results for OCM denoised image DN value between the strip or non-strip line values are used as reference and denoising results of destriped lines are compared to these references.

7.7.1 HySI Images

Standard deviation of the reservoir is measured at two main locations. One within the reservoir. The standard deviation of this part should reduce [14]. From Table 6.5 (UP) it can be seen that SURE-LET method out performs the other two methods in terms of reducing the standard deviation. Reduction in standard deviation of the reservoir is considered as significant improvement in the image quality.

The second locations is at the edge of reservoir. Standard deviation at the edges measures the edge sharpness and thus, should be preserved [14]. From the Table 6.5 DOWN it can be observed that after applying the denoising method the reservoir edges preserved. **Here, BLS-GSM method performed better for three bands and SURE-LET performed better for 64th band**

But visually results shows, Table 6.6-6.8, that SURE-LET image has less ringing artifacts as compare to other two methods. Though BLS-GSM performs better in terms of standard deviation at the edges but visually it gives image full of blocks and artifacts.

7.7.2 Simulated Image results

Table 6.10 shows the MSE and PSNR results for simulated image. From the results it can be seen that SURE-LET method performs better than other two methods. BLS-GSM performed better at the edges for reservoir, but as mentioned the visual quality was very poor for this method. This point can be strongly justified with simulated image results. In simulated image both, clean and denoised images are available MSE and PSNR can be measured. BLS-GSM

has poor performance in terms of MSE and PSNR, which is mainly due to the ringing artifacts. On the other hand, ProbShrink approach has much better performance as compare to BLS-GSM. But SURE-LET out performed with its MSE minimization function. The results are shown for different noise level. Although in practical scenario 60 db noise level means too much of noise and is hardly seen, but still it is included to gauge the performance of denoising.

In order to show the performance of the three methods for all the bands MSE and PSNR are plotted for one class in all the 64 bands. Table 6.12-6.13 shows the plot for MSE and PSNR for all the 64 bands. This shows that SURE-LET has better performance in all the wavelengths and no other method is near to its results.

Finally, in Table 6.14 visual results of one band of simulated image is shown applying three denoising methods. From visual inspection it can be seen that SURE-LET produces less ringing artifacts in reconstructed image.

7.7.3 OCM images

As mentioned in section 6.7, OCM results are verified by measuring the standard deviation of the homogeneous area. The images of the OCM sensor are of Goa region, a coastal state of India (Ref. Chapter 3), which has ocean in half of the scene. Because water can be considered as smooth area, the standard deviation of it can be measured to check the performance of denoising method.

But results obtained are not satisfactory. SURE-LET method completely failed to remove strips from the images. Visual interpretation shows that strips exist as it was before destriping. Even other two methods, ProbShrink and BLS-GSM has same results, they are unable to remove strips from the images. It is clearly visible from Table 6.15 (chapter 6).

The results obtained for OCM images is due to the nature of noise present in OCM images. SURE-LET method denoises the images contaminated with $AWGN$ only [3, 16].

7.8 How to estimate the noise level when no sensor parameter is available?

Before denoising the image it is required that the denoising function should know about the noise statistics. If denoising function does not know the noise level in the image then it is very likely that the important edge information could be lost. In other words without noise level estimation denoising function may behave like a low pass filter, which penalize the edges considering it as noise.

After a rigorous literature survey [2, 14, 3, 16, 7, 19] and the recommendation of SURE-LET and ProbShrink developers in this research work median estimator developed by [7] is used. The estimator can be expressed with following equation:

$$\sigma = MAD(|w_1^{HH}|)/0.6745 \tag{7.1}$$

Where, $MAD(|w_1^{HH}|)$ is a Median Absolute Deviation (MAD) and $w_1^{HH})$ is coefficients of wavelet HH_1 subband. Table 6.4, shows the result obtained using the MAD function. The average error in the estimation of noise is $+/-0.291$. The results are quite satisfactory and hence can be used in this research work.

7.8.1 Why median estimator estimates the noise?

It is very important to understand that why the expression 6.1 is able to estimate the noise? The answer lies in three factors:

1. Wavelet HH subband w_1^{HH}
2. MAD, Median absolute deviation
3. 0.6745

Let us begin with HH_1 subband. w_1^{HH}. In wavelet domain, the highest frequency of the signal stayed in HH_1 subband. HH means High-High subband i.e. subband whose coefficients are obtained by passing $2-D$ image component from High pass, where filter is basically the wavelet function. The term 1 used in HH_1 is level 1 decomposition. Thus, in wavelet domain highest frequency component stays in HH subband of level 1 [2]. Another fact is, this subband mainly contains noise, which is because of the fact that noise has high frequency components. So, measuring the HH_1 subband means measuring the noise.

For any data set $X1, X2, ..., Xn$ the MAD is defined as the median of the absolute deviations from the data set's median [36]:

$$MAD = median(|X_i - median_j(X_j)|) \tag{7.2}$$

MAD is used in estimating the noise because it is measure of statistical dispersion, measure which is a more robust estimator than standard deviation [36]. This is because standard deviation is biased for large deviations of samples from the mean, which means outliers can influence the results of standard deviation heavily. On the other hand, in MAD the magnitude of the distances of a small number of outliers is irrelevant and thus does not influence the results.

0.6745, this magic number is introduced by [7]. The motivation is, "if μ_n are N independent Gaussian random variables of zero mean and variance σ^2 , then $E(MAD(|\mu_n|)) \approx 0.6745\sigma$. [2]." Which is a valid assumption for $AWGN$ noise [2].

Understanding of all the above factors is the answer to the question that why median estimator estimates noise? Step by step the process of estimating noise can be explained as:

1. Go the place where noise is present, HH_1 subband.
2. Approximate the noise statistics, 0.6745σ
3. Measure the noise, Equation 6.1.

7.9 Results of denoising

7.9.1 HySI Results: Why BLS-GSM out performed for preserving edge part of the reservoir?

SURE-LET performed well for denoising the reservoir but has it preserved the edges? From Table 6.6(DOWN) it can be seen that BLS-GSM has better performance for three bands as compare to SURE-LET, which perform better only for Band 64th. Is it right to conclude that SURE-LET does not preserve edges? No!! Actually, BLS-GSM is not preserving the edges. BLS-GSM is a wavelet domain approach and as mentioned in section 6.1, wavelet based methods can produce ringing artifacts if they fail to reconstruct the image properly [5, 2]. BLS-GSM technique produces maximum artifacts in the reconstructed image as compared to other two methods, see Table 6.6-6.8. Ringing effects are basically false edges. When denoising method reconstructs the image, it tend to preserve the edges by computing its statistics. BLS-GSM method is wrongly performing this job and hence producing false edges. **These false edge increases the standard deviation measure, which deviate the results and shows BLS-GSM performing better.**

Why ProbShrink approach did not perform better than SURE-LET? The reason lies behind how denoising function for ProbShrink was formed. The ProbShrink approach is computes the statistics of the neighborhood pixels by using Markov Random Fields (MRF) [14]. MRF technique is widely used for incorporating the neighborhood information in the function to obtain better results [2]. But the problem with MRF based approaches is smoothness in reconstructed image [2]. **MRF may smooth the resultant image and hence, loss of information. It is because of this smoothness factor, ProbShrink approach did not perform better than SURE-LET.**

7.9.2 Why denoising method failed to remove strips from OCM images ?

To understand the reason of failure for denoising method it is required to understand two main concepts:

1. Denoising method structure
2. OCM noise type

Let us take these concepts one by one.

Denoising methods taken in this research work, both for denoising purpose and for comparison purpose, are build to remove quantization noise from the images [14, 3]. The quantization noise is basically a random noise, which can be proved by understanding the quantization process [36]. In the quantization process the samples has error that has upper bound of $\pm\frac{1}{2}$ LSB(Least Significant Bit), which means the distance between the successive levels [36]. Figure 6.2 shows the broad view of quantization process and error terms. As shown in Figure 6.2 quantization error can be found by subtracting sampled analog

signal from digitized signal i.e. (b) from (c) (in Figure 6.2) [36]. This shows that digital output shown in (c) is equivalent to sampled analog signal (b), which is still analog, plus quantization error shown in (d) [36]. An important realization of this analysis is the appearance of quantization error as random noise.

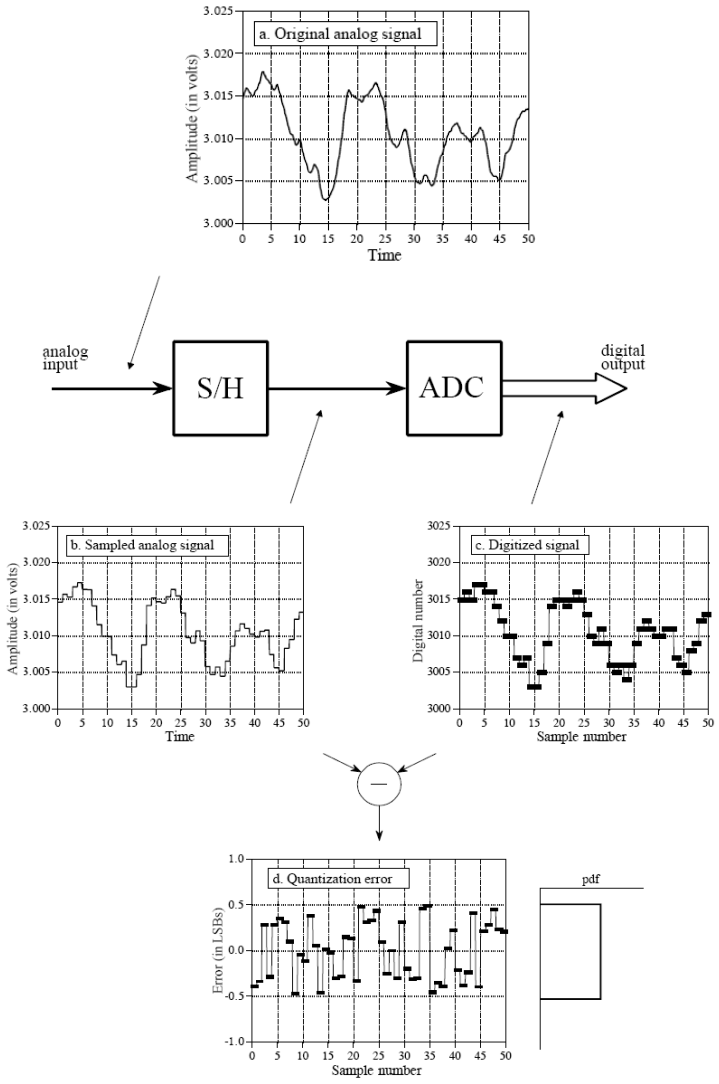

Figure 7.2: Shows the quantization process: (a) Original analog signal, A/D converter (b) Sampled analog signal (c) Digitized signal (d) Quantization error Source: The image is directly taken from (36)

"Most often quantization error is nothing more than the addition of a specific amount of random noise to the signal [36]". This helps to build the noise model for quantization as this additive error is uniformly distributed between $+/-$ $frac12$ LSB, has zero mean and $frac1\sqrt{12}$ standard deviation. The denoising method is build to remove this type of noise from the images.

Now, let us also see the type of noise present in OCM images. OCM sensor as mentioned in Chapter 3 is Ocean monitoring sensor (OCEAN COLOR Monitor)

used mainly for monitoring the ocean surface [29]. When OCM sensor pass through the earth surface the CCDs are used to acquire the irradiance. Due to the different characteristic of earth and water surface CCDs has different response to both the surfaces [29]. When sensor leaves the earth surface and enters the ocean surface i.e. it just start measuring ocean surface the CCDs are still charged to high values. (Earth has high irradiance as compare to ocean.) The CCDs due to practical constraint can not be designed to immediately go to low values [36, 29]. The process is slow and induces strips in the acquired image. Because it happened due to sensor design constraint, hence specific to sensor to sensor and therefore known as systematic error or noise.

It is very obvious that the denoising methods which are build to deal with random noise can not remove systematic error.

Note: Before starting this work we realized this fact and the test done on OCM images prove, the theory behind our justification built while developing the denoising function in Chapter 5.

7.10 Number of parameters in denoising function

In equations 5.9-5.13 (section 5.2, chapter 5), it was shown that how to linearly represent the denoising function. This linear representation of denoising function is known as linear expansion of threshold (LET).

As mentioned in section 5.1, the soft thresholding method is used in this research work. But The soft thresholding as shown in figure 7.4 has two drawbacks:

1. The shape of the soft thresholding function is not flexible, which means dependency on the parameter T is very high [3].

2. The dependency of soft thresholding function on parameter T is not linear in nature [3]. This means to minimize the denoising function non-linear function has to be used [3].

The denoising function suggested by the [3] is DOG function shown in equation 5.13. The DOG function because of its fast decaying nature ensures linear behaviour that is close to the identity of large coefficients, which allows to represent denoising function more flexibly as compare to the soft thresholding function, see figure 7.4 [3]. From equation 5.9-5.13, it can be seen that the total dependencies on the SURE denosing function are the number of linear coefficients a_k and the parameter T [3]. This overcomes the draw backs of soft thresholding method.

7.10.1 Effect of K

Let us see the effect of number of coefficients on the denoising function $\theta(y)$ shown in equation 5.13. With only one coefficient i.e. when $K = 1$, denoising function takes the following form:

$$\theta(y) = a_1 y \tag{7.3}$$

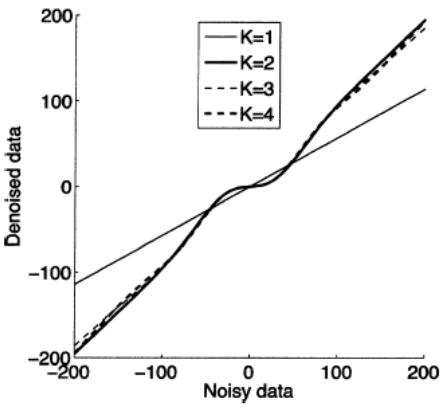

Figure 7.3: Shows the shape of denoising function in a particular subband for various k and optimized a_k and T. Source: (3)

Equation 7.3 is a linear pointwise function, minimization of this function using equation 5.8 will provide [3]:

$$a_1 = 1 - \frac{\sigma^2}{\langle y^2 \rangle} \tag{7.4}$$

Equation 7.4 is commonly known as James-Stein estimator [3, 16]. From figure 7.3 it can be observed that function with $K = 1$ transition between low SNR and high SNR coefficients is poor [3]. This is an important property of soft thresholding function, see Figure 7.4. Thus, value of K has to increase.

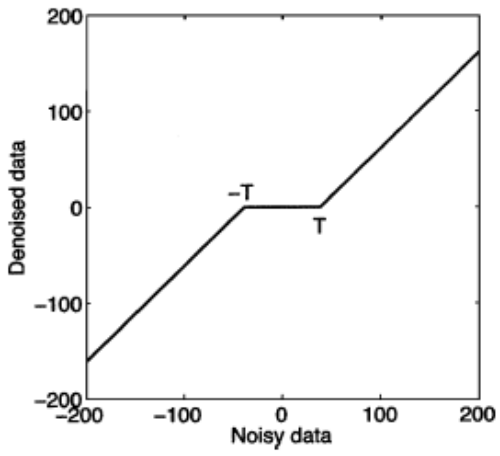

Figure 7.4: Shows the shape of denoising function in a particular subband for various k and optimized a_k and T. Source: (3)

From figure 7.3, it can be seen that for $K \geq 2$ the denoising function is not sensitive to the change [3]. This shows that $K = 2$ is the sufficient number to built a denoising function linearly [16, 3].

Chapter 8

Conclusion

"Waiting is a trap. There will always be reasons to wait. The truth is, there are only two things in life, reasons and results, and reasons simply do not count."
–Dr. Robert Anthony quotes

This chapter concludes the results of the methods discussed in chapter 5 on three data sets used in this research work. The chapter is outlined in such a way that each section is an answer to research question mentioned in chapter 1. Answer to these questions is given by the conclusion remarks.

8.1 What is the suitable wavelet family, support size and vanishing moment for the given wavelet?

Though best wavelet basis, support size and vanishing moment are subjective issues and depends upon the application, still some general points can be made and are as follows:

1. Visual quality of the reconstructed image is sensitive to smoothness of the wavelet filter. The importance of smoothness can be understood by assuming an error ϵ, which is added to coefficient and will add the $\epsilon\psi_{j,k}(x)$ component to the reconstructing signal *where ψ is a wavelet filter.* Now, if ψ i.e. wavelet is smooth then the error term $\epsilon\psi_{j,k}(x)$ is also smooth [2], which ensure, less visual artifacts or ringing effects in the reconstructed signal.

2. Symmetry of wavelet filter ensure the orthogonality and produce sparse coefficients [2].

3. For some applications more emphasis is on the coefficients properties, visual results are not required [34]. For example, segmentation method developed in this research work map the coefficients to image space, no reconstruction is done. In these type of applications, vanishing moment and support size depends upon the nature of coefficients required to map to image space.

8.2 What is the most suitable decomposition level for the given problem?

For wavelet domain, entropy can measure the edge information present in the image. After decomposing the the image, if entropy of the approximate subband LL is measured and if it is greater than 0, it means there are still edges in the approximate subband and further decomposition will not create a null vector for detail subbands [33].

Other then the edges, size of the image also influences the results. Small size images has less information as compare to large images in terms of discontinuity, except the case when image only contain smooth areas [33]. Thus, the entropy will reach to zero fast as compare to large images and level of decomposition will be less.

To justify the above point, part of the HySI band 50 is taken (75×75). The entropy for this subset found to reach zero at level 2. Thus, only first level of decomposition is appropriate.

From above discussion following conclusion can be made:

1. Entropy can be used to measure the best decomposition level.
2. Best decomposition level depends upon the edges in image and the size of image.

8.3 What is the technical applicability of SURE-LET for hyperspectral data?

Conclusion: Why no changes are required!!

As mentioned in chapter 5, (section 5.2 Equation 5.5 and 5.6) that SURE denoises the signal using function θ, which is a point wise function. Point wise functions are independently applied to each subband [3]. This means the data set has no influence on the processing only the decomposition filters and level of decomposition influences the results [2, 3].

Hence, it can be concluded that any method that works point wise in wavelet domain is independent of data set. And only noise type, wavelet filters and decomposition level can influence the results.

8.4 What technique should be adopted for reducing the number of spectral curves?

Why image segmentation is the answer to this question? and how it will work for fine resolution imageries?

This concludes, that if image is segmented using gray levels and is deteriorated by AWGN then each segment will be having equal effect of noise. These segments can be denoised by denoising only one pixel.

At image level, the whole image can be denoised by denoising only one pixel per segment. This is an important development and can reduce the processing time significantly. As seen in the results, 80% spectral curves are reduced.

The important point is only $AWGN$ fit to this type of model [36]. For other noise type the assumption may not be directly applied.

How this approach will work for fine resolution imageries? Answer is, methodology should be reconsidered. The approach to segment the image on the basis of gray levels is valid until the image is coarse resolution. But when images are fine in resolution then approach is required to be amended. It is because of the fact that at fine resolution more factors like, texture, shape, association etc. should also be considered, hence segment approach need to consider these factors.

With above point in mind this section finally concludes that the developed segmentation approach is valid for coarse resolution images only for fine resolution images more factors should be considered.

8.5 Which validation technique is suitable when no reference image and no sensor parameters are known?

When it is not possible to simulate the sensor acquisition system to produce the reference image [1], information of classes present in scene can be used. This is possible by using basic remote sensing principles. Interaction of objects and electromagnetic waves enable us to extract the behavior of some classes. Based on this behavior some reference can be set, which can be used to validate the results. The point can be justified with following examples:

1. HySI: As mentioned in Chapter 3 that the spatial resolution of HySI is 505m. At this coarse resolution, reservoir body, which covers large part of the image can be consider as homogeneous area. And according to [1] standard deviation of homogeneous are is mainly due to noise. This motivates to quantify the standard deviation before and after denoising the images.

2. Simulated image: For simulated image, clean, noisy and denoised version are present. This helps in quantifying the input MSE, input PSNR from clean and noisy images. And output MSE and output PSNR from clean and denoised version. By checking the improvement in output MSE and PSNR as compare to input MSE and PSNR performance of denoising function can be justified.

3. OCM: The noise in OCM is not random it is strip type noise. In strip type noise one advantage is to have one clean line between every two strips. This clean line is not affected by sensor's error and thus, can serve as reference line for the two neighboring strips. Measuring the standard deviation for three lines i.e. two strip and one clean line can serve as effective measure for quantifying the performance of denoising method.

The limitation of this method is the lack of knowledge about the class. If no information about the scene is available then it is required to visit the place, which some times not possible. In that case some classes can be identified using spectral library. Care should be taken while selecting the classes for spectral library match, as spectral signatures are available for pure classes only.

Chapter 9

Recommendations

"In research, the horizon recedes as we advance, and is no nearer at 60 than it was at 20. As the power of endurance weakens with age, the urgency of pursuit grows more intense... and research is always incomplete." **– Mark Pattison (1875)**

In this thesis, powerful wavelet domain denoising method to suppress noise of hyperspectral imageries is addressed. In the whole thesis, efforts have made to present the method through our original interpretations, pictorial representations, results, and conclusions. But for every ending there is a new beginning waiting. There is always a scope for development and this chapter focuses on elevating and improving the developed method. In the following section the recommendations for enriching the method is discussed.

9.1 The new thinking

Real life seems to have no plots.

Broadly, any denoising method can be designed in three main steps and the broad view of these steps is seen in this thesis. These steps are:

1. **Identify the Domain:** The denoising method may or may not be done in spatial domain or some mathematical domain like Fourier or wavelet or ridgelets. Before designing any denoising function it should be decided first, as lot many technical things depends upon it.

2. **Noise Level Function:** To preserve the information of images noise has to be estimated before applying denoising function to it. This part also covers the type of noise handled by denoising function and some basic statistics related to it.

3. **Denoising function:** Denoising function is a judge, which uses all the information available about the image and noise. Based on these information decides if a particular pixel (or coefficient in frequency domain) is noisy or not.

The three steps in this thesis are wavelet domain transformation, MAD estimation and SURE-LET denoising. While working on these steps I realized the need to use other methods as well, which is presented in this section as recommendations. The following sub-section covers these points in more detail.

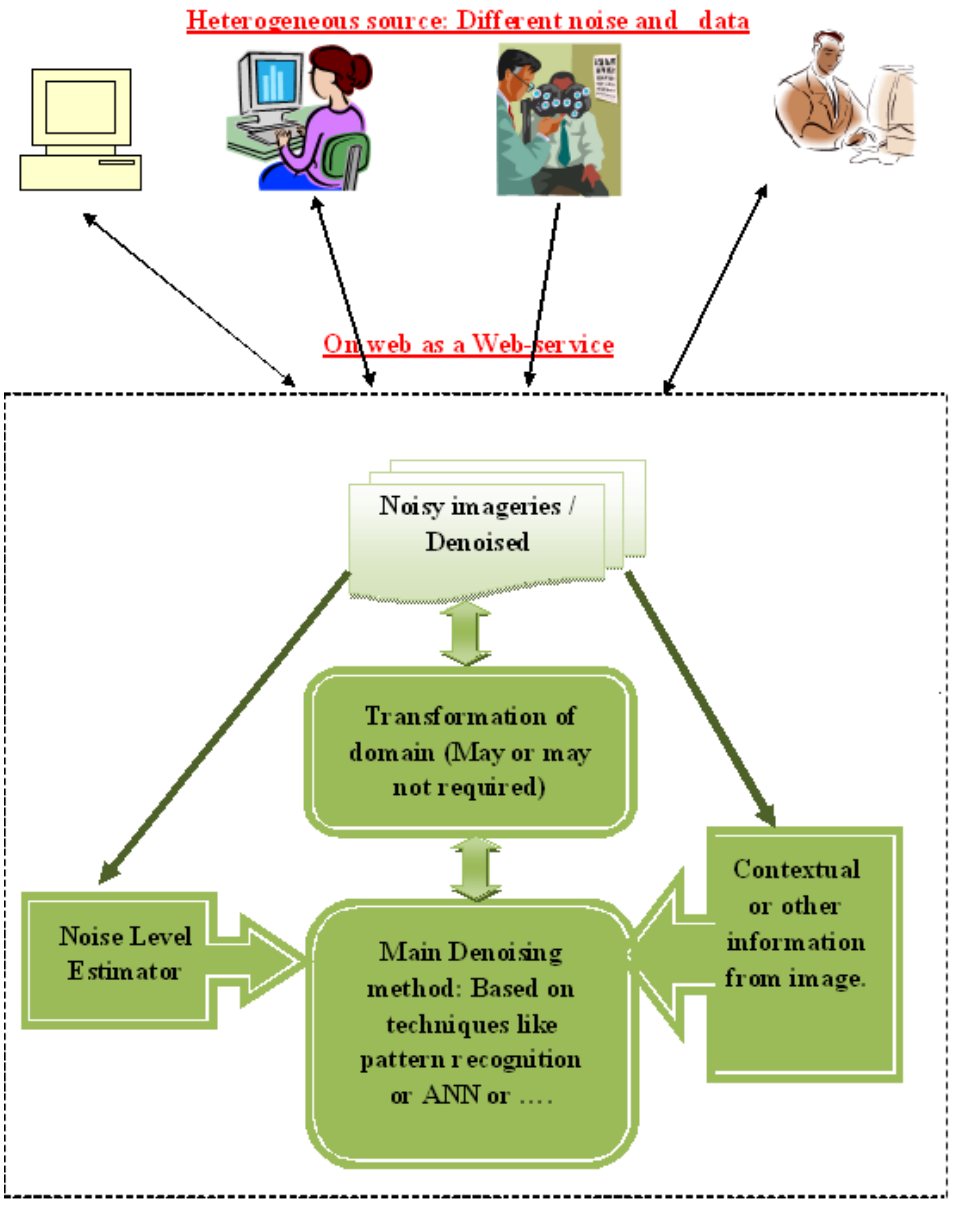

Figure 9.1: Shows the braod view of recommended denoising method

9.1.1 Independence from Noise and Data

The developed image denoising method focuses on removing $AWGN$ noise. The first recommendation is to overcome this constraint by developing method that

can tackle any type of noise (as discussed in chapter 1) present in images. The task is very hard because the noise type constraint mainly comes with the constraint in data sets. Specific data sets are degraded by some specific type of noise. To tackle all type noise (as mentioned in chapter 1) the denoising method should be able to take up different types of data sets, irrespective of their dimensions, wavelength and acquisition system. The idea is to make a generic denoising method that can denoise data from heterogeneous sources.

9.1.2 Identify domain :

The developed denoising method is wavelet based method, which more technically is a mathematical space. The second recommendation is to utilize other spaces or machine learning techniques to develop the denoising method. This may cover SVM based techniques or ANN or other pattern recognition techniques. MRF based techniques, which delivers very important contextual information can be integrated with denoising function for better performance. The idea is to elevate the power of denoising method so that it can recognize the noisy components more intelligently, which may save the information that sometimes penalized while denoising the images.

9.1.3 Noise level estimation

The main input to any denoising method is the estimation of noise level present in images. This estimation is a soul of any denoising method and should be properly designed. Especially for remote sensing images, where image information and noise changes with wavelength. In this research work noise level is estimated with Median Absolute Deviation. Other noise estimation techniques [1] can be used or developed. The idea is to estimate the noise level in better way. And as recommended, if the denoising method is developed for all types of noise (As mentioned in chapter 1), then work of noise level estimator becomes more important and complex.

At the end I also felt that there is no standard tool available to denoise the images. One solution can be to have a web-service that can take data from different sources and denoise it. The whole idea is shown in Figure 9.1.

References

[1] C.Liu, R.Szeliski, S.Bing, C.Lawrence, W.Freeman, "Automatic Estimation And Removal Of Noise From a Single Image" *IEEE Transaction on Pattern Analysis And Machine Intelligence*, Vol.30,No.2,pp.299-314, February 2008.

[2] A. Pizurica , "Image Denoising using wavelets and spatial context modeling", Research Thesis, Ghent University,2002.

[3] F.Luiser, T.Blu, and M.Unser,"A new SURE approach to image denoising: Inter-scale orthonormal wavelet thresholding," *IEEE Transaction on Image Processing*, Vol.16,No.3,pp.593-606,March 2007

[4] H.Othman and S.Aian, "Noise Reduction of Hyper spectral Imagery Using Hybrid Spatial-Spectral Derivative Domain Wavelet Shrinkage", *IEEE Transaction On Geosciences and Remote Sensing*, Vol.44,No.2, pp.397,February 2006.

[5] S.Mallat,"A Theory for Multiresolution Signal Decomposition The Wavelet Representation,"*IEEE Transaction on pattern Analysis And Machine Intelligence*, Vol.11,No.7,pp.674-693,July 1989.

[6] M.Shapiro,"Embedded Image Cosing Using Zerotrees of Wavelet Coefficients," *IEEE Transaction on signal processing*, Vol.41, No.41, pp.3445-3462,December 1993.

[7] D.L.Donoho and I.M.Johnstone, "Adapting to unkown smoothness via wavelet shrinkage," *J.Amer. Statist. Assoc.*, Vol.90, No.432,pp.1200-1224, December 1995.

[8] S.G.Cheng, B.Yu, and M.Vetterli," Adaptive wavelet thresholding for image denoising and compression," *IEEE Transaction on Image Processing*, Vol.9,No.9,pp.1135-1151,September 2000.

[9] N.G. Kingsbury, "Complex wavelets for shift invariant analysis and filtering of signals," *J.Appl. Comput. Harmon. Anal.*, Vol.10,No.3,pp.234-253,May 2001.

[10] E.P.Simoncelli and E.H.Adelson,"Noise removal via Bayesian wavelet coring," *In Proc. 3rd Int. Conf. Image Processing,* Lausanne, Switzerland, Vol.I,pp.379-382,1999.

[11] E.J.Candes,"Harmonic analysis of networks," *Appl. Comput. Harmoni. Anal.*,Vol.6,pp.197-218,1999.

[12] L.Sendur and I.W.Selesnick, "Bivariate shrinkage functions for wavelet-based denoising exploiting interscale dependency," *IEEE Transaction on Signal Processing*,Vol.9,No.11,pp.2744-2756, November 2002.

[13] J.Portilla, V.Strela, M.J Wainwright, and E.P. Simoncelli, "Image denosing using scale mixtures of Gaussian in the wavelet domain", *IEEE Transactions on Image Processing*, November 2003,Vol.12, No.11, pp.1338.

[14] A. Pizurica and W.Phillips, "Estimating the probability of the presence of a signal of interest in multiresolution signal, signal and multiband image denoising", *IEEE Transactions on Image Processing*, Vol. 15, No.3,pp.645-665,March 2006

[15] S.M.M Rahman, M.O Ahmads and M.N.S Swamy," Bayesian Wavelet-Based Image Denoising Using the Gauss-Hermite Expansion", *IEEE Transactions on Image Processing*, October 2008, Vol.17, No.10,pp.1755.

[16] T. Blu and F. Luisier, "The SURE-LET Approach to image Denoising", *IEEE Transactions on Image Processing*, November 2007, Vol. 16,No.11,pp.2778.

[17] Jose.A, Luis Mancer, and J.Portilla,"Image Restoration Using Space-Variant Gaussian Scale Mixtures in Over complete Pyramids", *IEEE Transaction on Image Processing*,Vol.17,No.1,January 2008.

[18] Buyue Zhang, and Jan P.Allebach,"Adaptive Bilateral Filter For Sharpness Enhancement And Noise Removal," *IEEE Transaction on Image Processing"*,Vol.17, No.5,May 2008.

[19] Y. Hel-Or and D. Shaked, "A Discriminative Approach for wavelet Denosing" , *IEEE Transactions on Image processing*, April 2008,Vol.17,No.4,pp.443.

[20] N.Otsu,"A Threshold Selection Method from Gray-Level Histograms", *IEEE Transactions on Syst. Man Cybern."*, Vol.9, No.9 pp.62-66, 1979

[21] S.G Chang and Martin Vetterli, "Spatial Adaptive Wavelet Thresholding For image Denoising", *IEEE Transaction on Image Processing*, Vol.9,No.9,September 2000.

[22] H.Choi and R.G.Baraniuk," image segmentation using wavelet-domain hidden Markov models",*IEEE Transaction on Signal Processing*, Vol.10,No.9,pp.1309-1321,September 2001.

[23] B.Kim , J.Shim, D.Park,"Fast image segmentation based on multi-resolution analysis and wavelets", *Pattern Recognition letters, Elsiver Computer Socity.* pp. 2995-3006, 2003.

[24] O.Feron And A.M Djafari,"Image Fusion and Unsupervised joint segmentation using HMM and MCMC algorithm", *Sub. Jornal of Electronic Imaging*, April 2004.

[25] H.Snoussi and A.M Djafari,"Fast joint separation and segmentation of Mixed Images",*Journal of Electronic Imaging*, Vol.13, No. 2, April 2004.

[26] M.Figueiredo,"Bayesian Image Segmentation Using Wavelet-Based Priors", *IEEE Computer Society Conference on Computer Vision and Pattern Recognition - CVPR'2005 (to appear)*

[27] A.Ertrk and S.Ertrk,"Unsupervised Segmentation of Hyperspectral Images Using Modified Phase Correlation", *IEEE GEOSCIENCE AND REMOTE SENSING LETTERS*, Vol.3, No.4, pp.527, OCTOBER 2006.

[28] D.Benot, B.Alexandre and, B.Charles," Fast Wavelet based Ultrasound Image Segmentation for Liver Vessels Extraction", *Presented at: Computer Aided Surgery around the Head (CAS-H), Leipzig*, February 6-9, 2008. Accepted in: 5th International Conference on Computer Aided Surgery around the Head,2008.

[29] Indian Satellite Information, Source: "http://www.isro.org/satellites/allsatellites.aspx", Accssed On January 5, 2010.

[30] Mathematics of change in basis, "http://en.wikipedia.org/wiki/Change_of_basis", Accessed On January 11, 2010.

[31] Robi Polikar,"Online Tutorial on Wavelets" Source: "http://users.rowan.edu/ polikar/WAVELETS/WTtutorial.html" Accessed On January 11, 2010.

[32] C.stein,"Estimtion of the mean of a multivriate normal distribution," *" Ann. Statist."*, Vol.9, pp.1135-1151,1981.

[33] Coifman, R.R., M.V Wickerhauser, "Entropy-based algorithms for best basis selection," *IEEE Transactions on Information Theory*, vol. 38,pp.713-718,1992.

[34] N. Bhatia, A.Kumar, V.A Tolpekin, "Automatic Segmentation of Image Using Orthonormal Wavelet Transform," *SUBMITTED FOR PUBLICATION TO: IETE, manuscriptID* $IETEJR_572_09$, OCTOBER 24, 2009

[35] Central limit theorem, "http://en.wikipedia.org/wiki/Central_limit_theorem", Accessed On January 11, 2009.

[36] S.Smith,"Digital Signal Processing A Practical Guide For Engineers and Scientists","An Imprint of Elsevier" 2006.

Appendix A

Publications

The method used in this research work is accepted and submitted to the following journals and symposium:

1. Paper accepted at: Indian Socity of Remote Sensing, ISRS Natinal symposium -2009, Nagpur. Under the topic "Hyperspectral image denoising inter scale orthonormal wavelet shrinkage". Authors: Nitin Bhatia, Anil Kumar, V.A Tolpekin

2. Manuscript submitted at: SUBMITTED FOR PUBLICATION TO IETE, manuscriptID IETEJR_572_09, OCTOBER 24, 2009. Under the topic "Automatic Segmentation of Image Using Orthonormal Wavelet Transform". Authors: Nitin Bhatia, Anil .Kumar, V.A Tolpekin